

PRODUCTION OF RADIOISOTOPES FOR MEDICAL  
AND INDUSTRIAL USES WITH CALIFORNIUM-252

A Thesis

Submitted to the Graduate Faculty of the  
Louisiana State University and  
Agricultural and Mechanical College  
in partial fulfillment of the  
requirements for the degree of

Master of Science

in

The Department of Nuclear Engineering

by

Rodney Dale Rogers  
B.S., Louisiana State University, 1971

August, 1973

126

Faint, illegible text, possibly bleed-through from the reverse side of the page.

DEDICATED TO  
my wife, Cynthia

## ACKNOWLEDGMENT

The author is deeply grateful for the indispensable advice and encouragement given by the many people who assisted in the preparation of this work. The assistance rendered by Dr. John C. Courtney, Dr. Robert C. McIlhenny, and Dr. Frank A. Iddings is especially appreciated.

The constant encouragement from my family and all that they have done for me is sincerely appreciated. To my wonderful wife, Cynthia, goes a special thanks for being so understanding and helpful.

## TABLE OF CONTENTS

	PAGE
ACKNOWLEDGEMENT.....	iii
LIST OF TABLES.....	vi
LIST OF FIGURES.....	vii
ABSTRACT.....	viii
 CHAPTER	
I. Introduction.....	1
General.....	1
Literature Review.....	5
II. Theory.....	6
Neutron Activation.....	6
Californium Thermal Flux Determination.....	12
III. Experimental Technique.....	15
Design and Construction of Irradiation Vessel.....	15
Selection of Experimental Radioisotopes.....	23
Description of Activation Procedure and Assembly.....	25
Preparation and Counting of Aliquot.....	34
Counting Equipment and Geometry.....	35
IV. Calculated and Experimental Results.....	37
Californium-252 Thermal Flux Distribution.....	37
Calculation of Theoretical Activity Yields.....	37
Determination of Counting Efficiency.....	37
Experimental Activity Yields.....	48
Average Activation Flux.....	54
V. Conclusions and Critique.....	56

	PAGE
REFERENCES.....	62
APPENDIX A.....	64
APPENDIX B.....	66
APPENDIX C.....	68
APPENDIX D.....	69
VITA.....	72

LIST OF TABLES

TABLE	PAGE
I. Neutrons from Spontaneous Fission of Californium-252.....	7
II. Quantities of Target Isotopes and Irradiation Times Used for Experimental Measurements.....	31
III. Calculated Activity Yields for Various Radioisotopes Produced with a $10^8$ Neutron-cm <sup>-2</sup> sec <sup>-1</sup> Flux.....	41
IV. Experimental Efficiencies.....	48
V. Absolute and Peak Efficiencies for 3-Inch by 3-Inch NaI(Tl) Crystal.....	50
VI. Experimental Activity Yields Extrapolated to Saturation for Various Moderator Thicknesses for 10 mg Cf-252.....	52
VII. Effective Activation Flux Determined from Experimental Activity Yields.....	55
VIII. Radioisotopes Showing Promise for Production with 10 Milligrams of Cf-252.....	58
IX. Medically Useful Radioisotopes Showing Promise for Production with 10 Milligrams of Californium-252.....	61

## LIST OF FIGURES

FIGURE	PAGE
1. Californium-252 Fission Spectrum.....	7
2. Maxwellian Velocity Distribution of Neutrons and Thermal Absorption Cross Section (for $1/v$ absorber).....	9
3. Final Vessel Design.....	19
4. Auxiliary Vessel Design.....	24
5. Total Cross Section <u>Versus</u> Neutron Energy for Na-23.....	26
6. Total Cross Section <u>Versus</u> Neutron Energy for Cu-63.....	27
7. Total Cross Section <u>Versus</u> Neutron Energy for In-115.....	28
8. Total Cross Section <u>Versus</u> Neutron Energy for Mn-55.....	29
9. Water Tank Storage and Activation Facility for Cf-252 Sources.....	33
10. Schematic of Counting System.....	36
11. Plexiglas Stand-off for Aliquot Counting.....	37
12. Thermal Flux Distribution Obtained from ANISN and DOT Code Calculations.....	40
13. A Comparison of Theoretical and Experimental Peak Efficiencies for a 3 Inch by 3 Inch NaI(Tl) Crystal with Point Source at 10 cm.....	49
14. Saturated Activity Yield <u>Versus</u> Moderator Thickness.....	51
15. Typical Gamma Spectrum Obtained for Cu-64 Sample.....	71



## ABSTRACT

An investigation of the feasibility of using 10 milligrams of californium-252 as a thermal neutron source for the production of short-lived radioisotopes was made. Data obtained from DOT and ANISN computer code calculations was used to predict the thermal neutron flux available. Theoretical activation yields based upon this predicted thermal flux were calculated for various radioisotopes producible by thermal neutron activation. Experimental measurements of actual activity yields were made using four isotopes whose cross sections were representative of the entire selected group of radioisotopes.

An irradiation vessel which served as a leak-proof container for all activations was designed and fabricated. One important feature of the vessel was that it allowed the thickness of moderator material around the source to be varied in order to optimize the activity yield. An auxiliary vessel smaller in volume was constructed to study the effect of increasing the target material concentration by sample volume reduction upon the activity yield. All experimental yields were determined by standard gamma spectroscopy using a 3-inch by 3-inch NaI(Tl) crystal.

The experimental results compared favorably with theoretical predictions. Variation of moderator thickness around the source, sample volume and target material concentration were found to be effective in optimizing the activation yields.

The effective activation flux from the 10 milligram californium-252 source was found to be sufficient for producing radioisotopes for industrial applications. However, because of high specific activity requirements, production of radioisotopes with medical applications was



found to be marginally feasible for only a few of the radioisotopes currently used.

### INTRODUCTION

#### General

Until the present, radioisotopes used in diagnostic procedures and radio-therapeutic treatment of patients, and in industrial radiography have predominantly been produced either with accelerators or by thermal neutron activation using nuclear fission reactors. The main reason for this has been the high neutron flux required. Other methods of obtaining neutron fluxes fall far short of producing useful quantities of radioisotopes. However, with the advent of californium-252, which decays by spontaneous fission, an intense isotopic source of neutrons became available. Each microgram of californium-252 emits  $2.34 \times 10^6$  neutrons per second. So it can be considered an alternative method to accelerators and nuclear reactors for the production of radioisotopes.

In nuclear medicine there is a definite need for radioisotopes which will provide improved diagnostic tests while at the same time minimize the radiation exposure that the patient receives. The National Academy of Sciences has recently issued a report on radiation exposure to the general population in which it emphasizes that steps should be taken to minimize unnecessary overexposure of patients. (1) This could be accomplished in the case of diagnostic medicine by being more selective in the choice of the radioisotopes used. One method of reducing the doses incurred would be to utilize isotopes which have shorter half-lives than the ones currently used at present. The problem with using these shorter half-lived isotopes is that until now, there was no practical means for

## CHAPTER I

### INTRODUCTION

#### General

Until the present, radioisotopes used in diagnostic procedures and radio-therapeutical treatment of patients, and in industrial radiotracing have predominantly been produced either with accelerators or by thermal neutron activation using nuclear fission reactors. The main reason for this has been the high neutron flux required. Other methods of obtaining neutron fluxes fell far short of producing useful quantities of radio-nuclides. However, with the advent of californium-252, which decays by spontaneous fission, an intense isotopic source of neutrons became available. Each microgram of californium-252 emits  $2.34 \times 10^6$  neutrons per second. So it can be considered an alternate method to accelerators and nuclear reactors for the production of radioisotopes.

In nuclear medicine there is a definite need for radioisotopes which will provide improved diagnostic tests while at the same time minimize the radiation exposure that the patient receives. The National Academy of Sciences has recently issued a report on radiation exposure to the general population in which it emphasizes that steps should be taken to eliminate unnecessary overexposure of patients.<sup>(1)</sup> This could be accomplished in the case of diagnostic medicine by being more selective in the choice of the radioisotopes used. One method of reducing the doses incurred would be to utilize isotopes which have shorter half-lives than the ones commonly used at present. The problem with using these shorter half-lived isotopes is that until now, there was no practical means for

a medical facility to receive them in usable quantities. Because of their short half-lives, these radioisotopes produced at a remote accelerator or in a reactor would have to be shipped with high activities. Upon delivery, the specific activity (activity per unit volume) of the radiotracer would be less as the result of decay during shipment. In most tracer studies using radioisotopes, a high specific activity is necessary to reduce the quantity of material injected into the patient. The amount of such chemicals injected must necessarily be small or insult to the body could occur. One approach to lessen this effect would be to chemically separate the radionuclide of interest from its daughter products before use. Another alternative would be for the diagnostic facility to have its own accelerator or reactor. The cost of this would be significant. In addition to equipment costs there is the expense of hiring health-physics personnel, trained operators and technicians. The problems of licensing and radiation hazards must also be considered. Californium-252 is now available for purchase through the Atomic Energy Commission at a price of \$10 per microgram plus encapsulation costs. For an investment of \$100,000, plus encapsulation costs of approximately \$2,000 to \$5,000, it is possible to purchase a 10 milligrams source. The maximum thermal neutron flux from this source in a water medium is approximately  $10^8$  neutrons  $\text{cm}^{-2}\text{-sec}^{-1}$ . This is sufficient to produce several shorter half-lived radioisotopes, along with some of the radioisotopes now used.

Medical tracers may be either radioactive or activatable. Radioactive tracers are almost exclusively used at present. However, activatable tracers could add a valuable dimension to tracer studies if

activation capabilities are available. An example of this would be the determination of the survival rate of red blood cells using radioactive chromium-51 as a radiotracer. The 0.32-Mev gamma ray emitted during its decay along with its relatively long half-life of 28 days prohibits its use for children or pregnant females. If isotopically enriched stable chromium-50 were used instead as a labeling agent and then activated to yield chromium-51 in vitro, this would eliminate all dose to the patient. There are numerous other stable isotopes which could be similarly used.

The question of just how important is it to optimize the production and use of radioisotopes in the diagnosis and treatment of patients might be raised. From surveys over the last 12 months it appears that greater than eight million patients benefited from nuclear medicine. Most of these cases (approximately 98%) involved diagnostic procedures using radioisotopes. <sup>(1)</sup> It is seen therefore that a relatively large number of people will benefit from even small improvements in the types of radioisotopes and procedures used. Perhaps the greatest benefit would be realized from improvements in the method of their production with respect to cost. At present, most nuclear medicine facilities obtain their radioisotopes from radio-pharmaceutical companies. The cost of these radioisotopes is high since the facility must buy quantities large enough to allow for the decay of the radioisotopes during shipping. This is not too severe a problem with some of the commonly used radioisotopes, but even the cost of these is quite high. These costs are of course passed on to the patient. Californium-252 has obvious advantages over the other two present methods of radioisotope production with respect to cost and convenience.



In industry, as in medicine, there is a definite need and potential market for short-lived radioisotopes. There are numerous instances where a longer half-lived tracer is not needed and its use involves an unnecessary loss of production time. It is in these short duration tracer studies that the advantages of a shorter half-lived radioisotope really become obvious. By using short-lived radioisotopes the hazards of a radiation spill or accident are greatly reduced. Should a spill occur, the response might simply involve waiting for the radioisotope to decay. With longer-lived radioisotopes it would be necessary to remove the contamination since too much time would be lost by waiting for the radioactive contamination to decay. During a tracer study the short-lived radioisotope is mixed in with the product. However, due to its short half-life there is no loss of product or contaminated product storage requirement as would be the case had a long-lived tracer been used. One other important advantage is that due to the short half-life of the tracer, larger quantities could be used in the tracer study. This greatly increases sensitivity of the technique. Both complexity and the cost of the detection system are thus greatly reduced. In general, the shorter the half-life, the higher is the energy of the radiation given off in decay. Therefore, the detection is made simpler due to the increased penetration of the higher energy radiation released.

The number of producible radioisotopes with industrial applications will more likely be larger than those with medical applications. This is because restrictions such as having a very high specific activity and being non-toxic are no longer screening factors.

Determining the feasibility of using this californium-252 facility to produce useful quantities of these short half-lived radionuclides for medical and industrial applications is the primary objective of this research.

### Literature Review

Currently much research is being performed with californium-252 as a neutron source. The uses of californium-252 for activation purposes deal almost exclusively with activation analysis. Only one research program involved with radioisotope production has been indicated to be in progress. <sup>(2)</sup> This research is being conducted by the Nuclear Engineering faculty at Pennsylvania State University. It was indicated that their department was hoping to obtain a series of intense californium-252 sources. However, the total quantity acquired as of December 1972 was 200 micrograms. <sup>(3)</sup> Their research would deal exclusively with short-lived medical radioisotopes and omits investigation of industrial radioisotope production. Several short-lived radioisotopes with possible medical applications were suggested in this article. The nuclides which can be produced by thermal neutron activation were included with other medically useful radioisotopes chosen for investigation. These radioisotopes, along with their possible medical applications, are listed in Table III. <sup>(2)(4)(5)</sup> Most of these medically useful radioisotopes will also have industrial applications. Other industrially useful radioisotopes producible through thermal neutron activation are also listed.

## CHAPTER II

### THEORY

#### Neutron Activation (6), (7)

When a stable isotope is placed in a neutron flux it will absorb neutrons, forming the next heavier isotope of the same element. This isotope may or may not be radioactive. Such a reaction is known as radiative capture or (n,  $\gamma$ ) reaction. If the new isotope is formed in an excited state, it usually falls to the ground state emitting a gamma ray. If the newly formed isotope is radioactive it will consequently decay by particle emission which may or may not be accompanied by gamma emission. It is these decay processes which allow the detection and thus the determination of the amount of radioactive material formed.

The amount of neutron absorption by a material is proportional to its absorption cross section  $\sigma_a$ . The absorption cross section is the probability that a neutron will be absorbed by the nucleus of an atom. It can be thought of as an effective target area through which a neutron must pass if it is to be absorbed by the nucleus of that atom. Absorption cross sections are tabulated for most isotopes of the various elements.

The absorption cross section is usually a complex function of neutron energy. Neutrons produced by a fission source, such as californium-252, can be represented by the "fission spectrum" shown in Figure 1. An analytic expression for this distribution is given by the Watt formula:

(8)

$$N(E) = 0.373 \exp(-0.88) \text{SINH}(2.0E)^{1/2}, \quad (2-1)$$



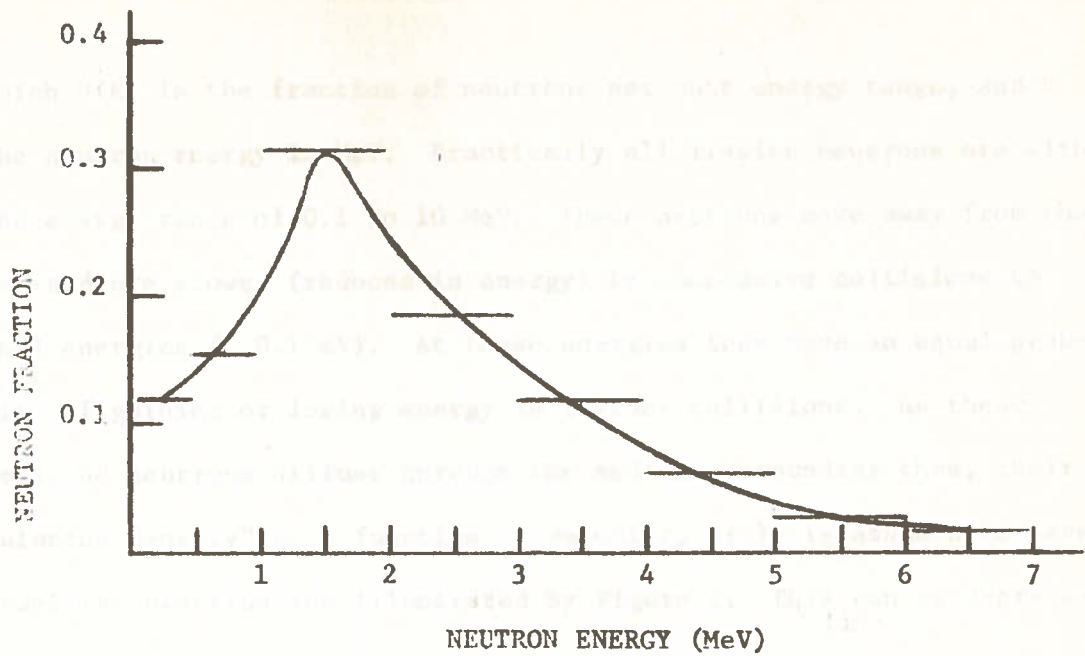


FIGURE 1. Californium-252 Fission Spectrum

TABLE I. NEUTRONS FROM SPONTANEOUS FISSION OF CALIFORNIUM-252

<u>Energy MeV</u>	<u>Neutrons/(sec)(g of nuclide)</u>	<u>Neutron Fraction</u>
0 - 0.5	$2.8 \times 10^{11}$	0.1165
0.5 - 1.0	$3.7 \times 10^{11}$	0.154
1.0 - 2.0	$7.6 \times 10^{11}$	0.317
2.0 - 3.0	$4.6 \times 10^{11}$	0.191
3.0 - 4.0	$2.8 \times 10^{11}$	0.1165
4.0 - 5.0	$1.6 \times 10^{11}$	0.0658
5.0 - 6.0	$5.6 \times 10^{10}$	0.0233
6.0 - 7.0	$4.0 \times 10^{10}$	0.0166
7.0 - 8.0	$1.3 \times 10^{10}$	0.00542
8.0 - 10.0	$9.9 \times 10^9$	0.00412
10.0 - 13.0	$2.2 \times 10^9$	0.00092
TOTAL	$2.4 \times 10^{12}$	

in which  $N(E)$  is the fraction of neutrons per unit energy range, and  $E$  is the neutron energy in MeV. Practically all fission neutrons are within the energy range of 0.1 to 10 MeV. These neutrons move away from the source and are slowed (reduced in energy) by successive collisions to thermal energies ( $< 0.1$  eV). At these energies they have an equal probability of gaining or losing energy in further collisions. As these thermalized neutrons diffuse through the medium surrounding them, their "population density" as a function of velocity,  $n(v)$ , is assumed to have a Maxwellian distribution illustrated by Figure 2. This can be expressed as

$$n(v) = N_0 \frac{4\pi v^2}{(2\pi kT/m)^{3/2}} \exp\left[\frac{-mv^2}{2kT}\right] \quad (2-2)$$

in which  $N_0$  = thermal neutrons per  $\text{cm}^3$

$m$  = neutron rest mass

$T$  = Temperature, °Kelvin

$k$  = Boltzmann constant =  $8.6 \times 10^{-5} \left(\frac{\text{eV}}{\text{°K}}\right)$ .

The most probable neutron velocity  $v_p$  may be found by setting the derivative of  $N(v)$  with respect to velocity equal to zero. The result is

$$v_p = \left(\frac{2kT}{m}\right)^{1/2} \quad (2-3)$$

For a neutron at  $20^\circ\text{C}$ ,  $v_p$  is equal to 2200 meters per second. It is for this velocity and the corresponding kinetic energy of 0.025 eV that thermal neutron absorption cross sections are tabulated.

The average velocity of these thermal neutrons is given by

$$\bar{v} = \frac{\int_0^\infty n(v) v dv}{\int_0^\infty n(v) dv} = \frac{\int_0^\infty \frac{4\pi N_0 v^3 \exp\left[\frac{-mv^2}{2kT}\right]}{(2\pi kT/m)^{3/2}} dv}{N_0} \quad (2-4)$$

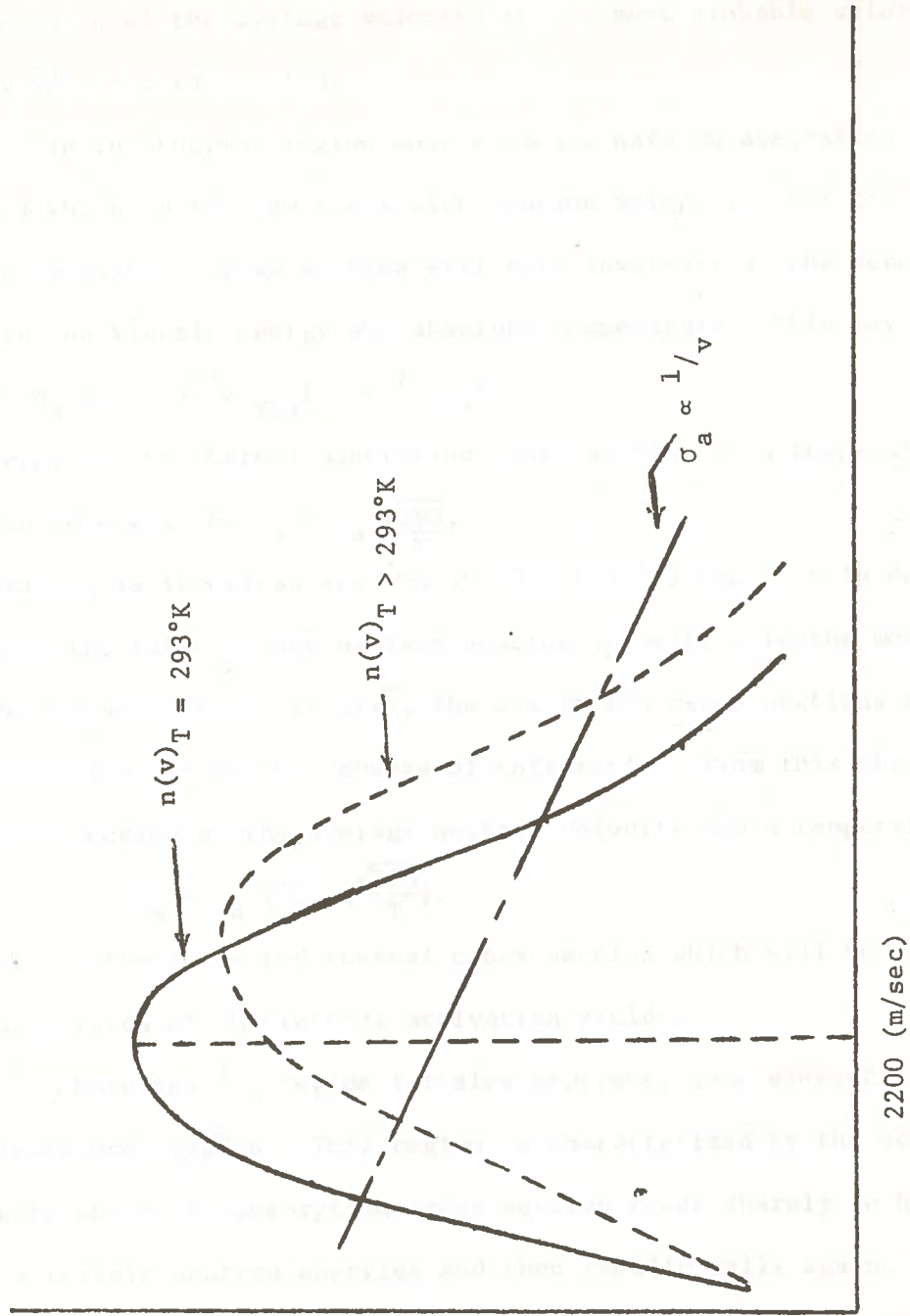


FIGURE 2. Maxwellian Velocity Distribution of Neutrons and Thermal Absorption Cross Section (for  $1/v$  absorber).

Upon integration this yields  $\bar{v} = \left(\frac{8kT}{\pi m}\right)$ . (2-5)

The ratio of the average velocity to the most probable velocity is therefore  $\bar{v}/v_p = 2/\sqrt{\pi} = 1.128$ . (2-6)

In the thermal region most elements have an absorption cross section which varies inversely with neutron velocity. For these elements the absorption cross section will vary inversely as the square root of both the kinetic energy and absolute temperature. This may be expressed as  $\sigma_a \propto 1/v \propto 1/(\text{KE})^{1/2} \propto 1/(T)^{1/2}$ . (2-7)

Therefore the thermal absorption cross section at a temperature other than 20°C will be  $\sigma'_a = \sigma_a \frac{\sqrt{293}}{T}$ , (2-8)

where  $\sigma_a$  is the cross section at 20°C (293°K) and T is in degrees Kelvin.

Since the ratio of the average neutron velocity  $\bar{v}$  to the most probable neutron velocity  $v_p$  is  $2/\sqrt{\pi}$ , the absorption cross sections at these two velocities are in the inverse of this ratio. From this the absorption cross section at the average neutron velocity and a temperature T is,

$$\bar{\sigma}'_a = \sigma_a \left(\frac{\sqrt{\pi}}{2}\right) \left(\frac{\sqrt{293}}{T}\right). \quad (2-9)$$

This is the corrected thermal cross section which will be used in the calculation of theoretical activation yields.

Above the  $1/v$  region for slow neutrons, some elements exhibit a "resonance" region. This region is characterized by the occurrence of peaks where the absorption cross section rises sharply to high values for certain neutron energies and then rapidly falls again. These resonance peaks for (n,  $\gamma$ ) reactions at low neutron energies are usually sharp. It is important to point out however that not all elements exhibit this type of behavior. Most nuclides of low mass number, do not exhibit resonance absorption to any appreciable degree.

Beyond the resonance region, absorption cross sections decrease steadily with increasing energy. It is in this "fast" neutron region that reactions other than the  $(n, \gamma)$  reaction become predominant. These include the  $(n, \alpha)$ ,  $(n, p)$  and  $(n, 2n)$  reactions. Since the purpose of this investigation is to determine the ability of californium-252 to produce radioisotopes by thermal neutron activation, fast neutron reactions will not be considered.

Because the absorption is a function of neutron energy and some nuclides exhibit significant resonance structure, the optimum spectrum for maximum activation will vary for different isotopes. For elements exhibiting no resonance absorption the highest thermal neutron flux would be desirable. For elements having large resonance peaks, it may be desirable to have the majority of incident neutrons at this resonance energy. This can be accomplished by placing varying thicknesses of moderator materials between the californium-252 source and the sample to be activated. The optimum amount of moderator may vary for different isotopes. If the isotopes selected for investigation can be classified according to similar cross section variation, a representative isotope from each category can then be selected. Using these representative isotopes, the optimum moderator thickness can be determined for each. Based on these findings predictions as to the optimum moderator thickness can be made for each isotope.

In the activation process, if a newly formed isotope is unstable it will decay at the same time it is being formed. If  $N$  is the number of nuclei of the new isotope, and  $N_0$  is the number of original target nuclei, a differential equation describing the rate of change of new



nuclei may be written. The rate of change of new nuclei is equal to their rate of formation minus their rate of decay as shown by

$$\frac{dN}{dt} = \phi N_0 \bar{\sigma}'_a - \lambda N, \quad (2-10)$$

where  $\lambda$  is the decay constant and  $\phi$  is the thermal neutron flux. The number of target nuclei  $N_0$  is given by

$$N_0 = \frac{6.023 \times 10^{23} \left(\frac{\text{Atoms}}{\text{Mole}}\right) * \text{Weight (grams)} * (\text{Abundance})}{A \left(\frac{\text{grams}}{\text{mole}}\right)} \quad (2-11)$$

The solution of this first order differential equation yields

$$\text{Activity} = N\lambda = \phi \bar{\sigma}'_a N_0 (1 - \exp[-\lambda t_a]). \quad (2-12)$$

The term  $t_a$  is the time of activation and activity is in disintegrations per second. This equation describes the build up of radioactive nuclei for irradiation of stable nuclei in a thermal neutron flux. The term  $(1 - \exp[-\lambda t_a])$  is known as the saturation factor. Irradiation for  $t_a$  sufficiently large so that  $\exp[-\lambda t_a]$  approximates zero will yield the saturation activity. Theoretical activation yields calculated using equation (2-12) must be considered as optimum yields possible for thin targets. The actual experimental yields may be lower due to flux depression and self-shielding effects.

#### Californium-252 Thermal Flux Determination and Distribution

The problem of determining the neutron flux distribution of a point fission source such as californium-252 is very complex. Treatment of this problem has been accomplished using a "two group Diffusion Theory combined with Age Theory" approach and the digital computer. A computer code which uses this approach, BWNP, is available for use by the Louisiana State University Nuclear Science Center. However, the

calculated flux distribution near the californium-252 source obtained by using this code is inaccurate. This results from the inadequacy of Diffusion Theory to treat the neutron flux as a function of energy in regions very near a neutron source.

For more accurate description of the neutron flux distribution in regions very near a neutron source the Transport Theory treatment must be used. Transport Theory is based upon the Boltzmann integrodifferential equation which is a neutron balance equation.<sup>(9)</sup> The exact solution to the transport equation cannot be obtained except in the simplest cases. Various computer codes which yield approximated solutions have been developed. The complexity of the solution increases with the degree of accuracy desired.

The solution of the one dimensional Boltzmann transport equation in slab, spherical or cylindrical geometry can be obtained using the ANISN digital computer code.<sup>(9)</sup> The source may be a fixed source, a fission source, or a subcritical combination of the two. Californium is a point fission source most easily treated in spherical geometry. The solution technique used in ANISN is an advanced discrete ordinance method. This code is not at present operational on the Louisiana State University digital computer. However, data obtained by ANISN calculations has been reported for a point californium-252 source.<sup>(10)</sup> These results will be used for comparative purposes.

DOT (Discrete Ordinates Transport) is a code which is now operational at Louisiana State University.<sup>(11)</sup> It is a general purpose discrete ordinates method which solves the energy dependent Boltzmann transport equation for two dimensional geometries. In calculations for a point californium-252 source the  $r,0$  geometry would apply.



The DOT and ANISN calculations yield the thermal flux as a function of distance from the source for the medium surrounding the source. The thermal flux magnitude at the surface of the source can be used to determine the theoretical thermal neutron activation yields for the various radioisotopes of interest.

In order to prevent contamination of the sample in the irradiation facility, a vessel would be leak proof and allow easy removal of the sample without the need for the vessel. Such a vessel treatment would allow the irradiated sample to be moved from the irradiation facility to the counting area without the need of a shield.

Determining the moderator thickness for optimum activation requires that the moderator thickness be varied while maintaining a reasonably constant, reproducible geometry for activation. If other variables which can cause flux variation are not held reasonably constant, there can be no correlation between the activation yield and thickness of moderator around the source.

Preliminary Design. For an ideal point californium-252 source, a spherical sample with the source surrounded by moderator at the center would theoretically be the optimum symmetrical geometry. This is true for a spherical geometry which maximizes flux utilization. For an unencapsulated

## CHAPTER III

### EXPERIMENTAL TECHNIQUE

#### Design and Construction of Irradiation Vessel

Design Criteria. Because of the limited funds available, cost is a strong consideration in the selection of materials for this investigation. For maximum production of radioisotopes, the construction materials used for the irradiation vessel must have low neutron absorption cross sections. Parasitic neutron capture can significantly reduce the available flux. Any construction materials must have a high resistance to radiation damage and be easy to fabricate.

In order to prevent contamination of the sample or the irradiation facility, a vessel which is leak proof and allows easy removal of the radioisotope after activation is needed. Such a secure containment vessel allows the activated sample to be moved from the activation area to the counting area with a minimum of hazard involved.

Determining the moderator thickness for optimum activation requires that the moderator thickness be varied while maintaining a reasonably constant, reproducible geometry for each activation. If other variables which can cause flux variation are not held reasonably constant, there can be no correlation between the activation<sup>o</sup> yield and thickness of moderator around the source.

Preliminary Design. For an ideal point californium-252 source, a spherical sample with the source surrounded by moderator at its center would theoretically be the optimum symmetrical geometry. This  $4\pi$  irradiation geometry would maximize flux utilization. For an encapsulated

source, which approximates a line source, cladding thickness at both top and bottom prohibits a spherically symmetrical flux. This is because of the much larger perturbation and absorption caused by the additional encapsulation material at the ends of the source as compared to the lateral surface. To avoid these perturbation areas, a cylindrical activation geometry was chosen. The flux in this cylindrical geometry is a symmetrical function of the radius but a non-symmetrical function of the height above and below the source. For this reason the variation in height for samples at different moderator thicknesses must be small. The method of maintaining a constant volume by decreasing the radius of the vessel wall was excluded from consideration. Although the height would have been held constant using this method, varying the radius of the vessel wall was considered unnecessarily tedious and expensive.

For the irradiation geometry chosen, the source during activation would be at the geometrical center of both the sample volume and moderator. The sample is annular in shape and its volume is given by

$$V = \pi(r_o^2 - r_m^2)h \quad (3-1)$$

in which  $r_o$  is the inner radius of the cylindrical vessel wall,  $r_m$  is the radius of the cylindrical moderator, and  $h$  is the height of the moderator and sample. For determining the sample size needed, a value of 0.5 inch was assigned as the maximum allowable variation in the height of the sample. This would mean a variation of 0.25 inches above and below the source as the moderator thickness is reduced. With this arrangement it was felt that the activation yield would be independent of the small variation in sample height and dependent only upon moderator thickness. To begin activation, the source must be inserted by lowering

it into the center of the moderator. The encapsulated source is 1.50 inches tall and 0.375 inches in diameter. A 0.5 inch hole drilled into the center of the moderator would allow easy insertion and removal of the source. The hole should be drilled to a depth which would allow the source to be geometrically centered while resting in its activation position. Using these source dimensions the minimum sample and moderator height was set at 1.7 inches and the moderator radius was limited to a 0.375 inch minimum. This allows 0.1 inch of moderator beneath and 0.125 inch around the source, thereby maintaining it completely within the moderator. The moderator material keeps the source and sample separated, and prevent leakage of the sample from the irradiation vessel. Adding this minimum sample and moderator height to the allowable variation of 0.5 inches would give the maximum moderator and sample height of 2.2 inches.

From the neutron flux distribution it is seen that after a distance of five centimeters of water the flux has begun to rapidly decrease (refer to Figure 12 in Chapter IV). For this reason the maximum moderator radius was chosen to be 2.0 inches. Thus, for the maximum moderator radius of 2.0 inches the corresponding sample and moderator height is 2.2 inches. For the minimum moderator radius of 0.375 inches the corresponding moderator and sample height is 1.7 inches. Since the sample volume is to remain constant, these maximum and minimum sample configurations must be equal in volume. There is only one radius for the inner wall of the vessel and one sample volume which can satisfy these conditions simultaneously. The method of calculating this vessel radius and volume are given in Appendix A. The required inner radius of the vessel



wall was calculated to be 4.138 inches. The corresponding sample volume is 1486 milliliters. This sample volume can be held constant simply by reducing the height of the moderator as it is reduced in thickness. As the moderator is reduced in size, the level of the sample drops. A large air gap is thus created between the top of the vessel and the surface level of the liquid. This is undesirable from a geometry standpoint. To eliminate the air gap a leak-tight top which could be moved up or down to maintain contact with the liquid surface must be constructed.

Final Design. The final vessel design which met all design criteria, especially ease of fabrication and low cost, is shown in Figure 3. Both the vessel and moderator materials are Plexiglas<sup>\*</sup>. This was the cheapest construction and moderator material because Plexiglas scrap at a cost of fifty cents per pound was readily available. In addition to being inexpensive, Plexiglas is almost equivalent to water with respect to its moderating properties. (7) Fabrication was relatively simple because of excellent machining properties of Plexiglas. Most of the fabrication was performed with a lathe and a drill press. The cylindrical moderator was turned from an irregular block of Plexiglas. The radius of the machined cylinder was 1.95 inches, slightly less than desired. Further improvising was required because the largest section of Plexiglas tubing available as scrap was 6.506 inches in diameter. This is somewhat less than the desired diameter of 8.27 inches, the diameter needed to keep the height variation of the sample volume to 0.50-inches. Therefore another determination of the sample volume and its height variation was made.

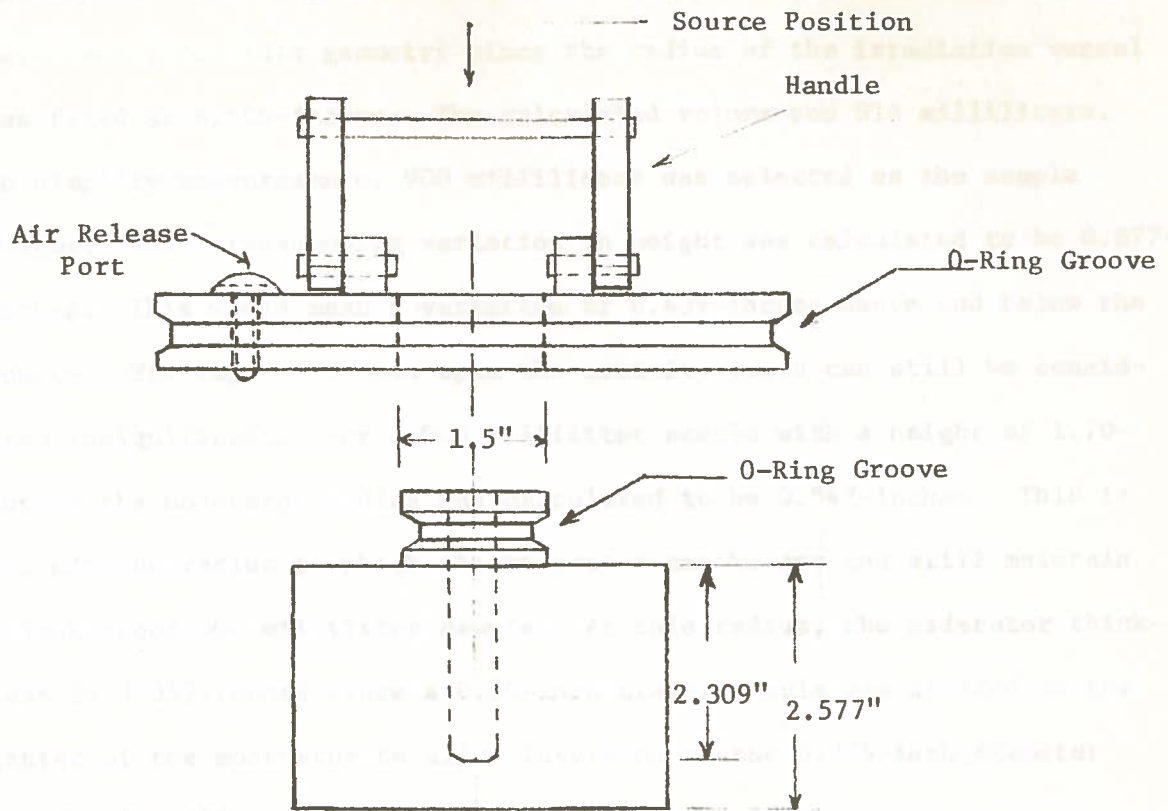
---

\*Registered trademark for acrylic sheet manufactured by Rohm and Haas Company

The top surface calculations are shown in Appendix B. The calculations were made for a cylindrical vessel with a diameter of 1.5 inches and a height of 2.577 inches.

To obtain the measurements, a 900 milliliter Erlenmeyer flask was selected as the sample vessel. The flask was modified to meet the design requirements.

The design of the vessel is shown in Figure 3. The vessel is a cylindrical vessel with a diameter of 1.5 inches and a height of 2.577 inches.



The bottom of the vessel was formed from a circular disk machined from aluminum. The diameter of the disk was 1.5 inches.

The vessel was then attached to the top of the vessel. The vessel was then attached to the top of the vessel.

The vessel was then attached to the top of the vessel. The vessel was then attached to the top of the vessel.

The vessel was then attached to the top of the vessel. The vessel was then attached to the top of the vessel.

The vessel was then attached to the top of the vessel. The vessel was then attached to the top of the vessel.

The vessel was then attached to the top of the vessel. The vessel was then attached to the top of the vessel.

The vessel was then attached to the top of the vessel. The vessel was then attached to the top of the vessel.

The vessel was then attached to the top of the vessel. The vessel was then attached to the top of the vessel.

The vessel was then attached to the top of the vessel. The vessel was then attached to the top of the vessel.

The vessel was then attached to the top of the vessel. The vessel was then attached to the top of the vessel.

The vessel was then attached to the top of the vessel. The vessel was then attached to the top of the vessel.

FIGURE 3. Final Vessel Design

The vessel was then attached to the top of the vessel. The vessel was then attached to the top of the vessel.

The appropriate calculations are shown in Appendix A. The calculations were easier for this geometry since the radius of the irradiation vessel was fixed at 6.506-inches. The calculated volume was 914 milliliters. To simplify measurements, 900 milliliters was selected as the sample volume. The corresponding variation in height was calculated to be 0.877-inches. This would mean a variation of 0.439-inches above and below the source. The impact of this upon the activity yield can still be considered insignificant. For a 900 milliliter sample with a height of 1.70-inches the moderator radius was calculated to be 0.547-inches. This is the minimum radius to which the moderator can be cut and still maintain a leak-proof 900 milliliter sample. At this radius, the moderator thickness is 0.357-inches since a 0.50-inch diameter hole was drilled in the center of the moderator to allow insertion of the 0.375-inch diameter californium-252 source.

The bottom of the vessel was formed from a circular disk machined from a 0.50-inch thick Plexiglas plate. Plexiglas cement was used to affix the bottom to the cylindrical wall of the vessel.

The circular disk forming the depressable top of the vessel was machined from 0.75-inch Plexiglas plate. It was machined to a radius which was less than the inner radius of the vessel wall. A 1.50-inch hole was drilled at the center and an O-ring groove was filed to a depth which would allow the top to slide up or down with the aid of a silicone vacuum grease.

A 0.75-inch section of the moderator was machined to 1.5-inches in diameter. An O-ring groove was turned with the lathe. Sandpaper was used to slightly enlarge the hole in the cover until a tight fit was



obtained. Once this moderator neck with its O-ring was inserted into the top, they composed a water-tight cover for the vessel. To allow the cover to be lowered to the level of a liquid sample, a hole for a 0.25-inch screw was drilled and tapped. This allowed the air to escape as the top was compressed down. A 0.25-inch plastic screw and fiber washer were inserted and tightened to form a leak-proof irradiation vessel. To remove the top after activation the plastic screw must first be removed. If the screw is not removed, the vacuum will prevent the removal of the top.

To assist in compressing and removing the top, a handle was constructed using 0.50-inch Plexiglas rod and Plexiglas squares. The two squares were drilled, centrally mounted and cemented to the top. These squares acted as a pivot point for the handle. The handle could be moved from its vertical position, thus allowing the source to be inserted into the moderator.

To assist in lowering the irradiation vessel into and removing it from the activation facility, three small Plexiglas squares were shaped to conform to the curvature of the vessel wall. Small holes were drilled in these squares before they were cemented flush with the lip of the vessel at 120 degree intervals. Nylon string was tied to each square to form a harness.

After experimentation with a particular moderator thickness was completed, the procedure of changing moderator thickness involved simply removing the moderator from the top and machining the portion below the neck to the desired thickness and corresponding height.

Design of Auxiliary Vessel. To estimate the effect of concentrating the target material, a smaller vessel was needed for determining the activity yields of smaller volume samples. These samples were to have the same amount of target material as contained in the 900 milliliter samples but in a reduced volume. It was felt that the expense of fabricating a vessel similar to the 900 milliliter vessel should be avoided if possible. Therefore it was decided that the 900 milliliter vessel should serve as an outer containment vessel. A smaller, less intricate vessel was constructed to contain the sample. It was made by removing the upper two-thirds of a polyethylene bottle and casting a paraffin cover to fit securely over the remaining bottom portion. An opening approximately equivalent to the diameter of the moderator was also incorporated into the mold. Thus the cover of the containment vessel could be depressed until the moderator was firmly in contact with the bottom of the smaller polyethylene vessel. In this position, the moderator was centrally located in the volume of the smaller vessel. Before depressing the cover of the containment vessel, water was added to surround the smaller vessel. Thus an activation geometry similar to that for the 900 milliliter samples was maintained.

For these activations a special moderator was turned on the lathe. With the moderator inserted, the volume of sample contained in the smaller vessel was 120 milliliters. A 0.5-inch hole was drilled in the center of the moderator to a depth which allowed the californium-252 source to be at the geometrical center of the sample volume when inserted. A radius of 0.603-inches was selected so that comparisons of the activity yields of 900 and 120 milliliter volume samples could be made at equiva-

lent moderator thickness. A schematic of the 120 milliliter vessel is shown in Figure 4.

#### Selection of Experimental Radioisotopes

Selection of radioisotopes for experimental investigation was based upon six criteria. First, for a radioisotope to be selected, its target material had to be either inexpensive or available at the Nuclear Science Center in sufficient quantities. Second, the activation cross section had to be large enough so that activities yielding good counting statistics could be produced. Third, it was desirable that the radioisotope be easily detectable, that is, have a gamma of high enough energy to be above the low energy scatter region. Being easy to handle from a chemistry standpoint and having a chemical form which is soluble in water is a fourth criteria. Fifth, a chemical inertness with respect to Plexiglas and rubber is mandatory. Sixth, it is desired that the radioisotopes selected be collectively representative of the cross section variation for the entire group of radioisotopes of interest. This would allow general predictions of the experimental yields which could be expected for each isotope.

Four broad classifications as to cross section were chosen. Group I included those radioisotopes whose cross section for production was constant, with little resonance absorption. Group II included those radioisotopes with production cross sections having a  $1/v$  behavior in the thermal energy region, with negligible resonance absorption. Group III included those which have  $1/v$  production cross sections, and also exhibit large resonance absorption in the region above 0.5-eV. Group IV





represented those radioisotopes whose cross section for production is  $1/v$ , with large resonance absorption at 1000-eV or greater.

The four nuclides selected for investigation which met these criteria were sodium-23, copper-63, indium-115 and manganese-55. These represented groups, I, II, III, IV respectively. The cross sections as a function of energy for these four nuclides are shown in Figures 5, 6, 7, and 8. <sup>(12)</sup> These are total cross sections and represent the combined scattering and absorption cross sections. The resonance peaks are for absorption rather than a combination of absorption and scattering. That is, the contribution of scattering reactions to the resonance peaks in the total cross section versus energy curve is negligible.

#### Description of Activation Procedure and Assembly

Preparation of Samples. For determining the optimum moderator thickness, samples were prepared in the irradiation vessel by mixing 870 milliliters of water with the desired amount of target material. After the target material was dissolved, the cover, with moderator in place, was compressed until the moderator was firmly in contact with the bottom of the vessel. An additional 30 milliliters of water was then added through the 0.25-inch hole in the vessel cover with a syringe. This approach was used to avoid losing a portion of the sample through the 0.25-inch vent hole. The vessel was then sealed by inserting and tightening the plastic screw and fiber washer.

For a comparison of activity yield as a function of target material concentration, the same quantity of target material as used in the determination of optimum moderator thickness was dissolved in the 120 milliliter vessel. After the paraffin cover was pressed into place, the

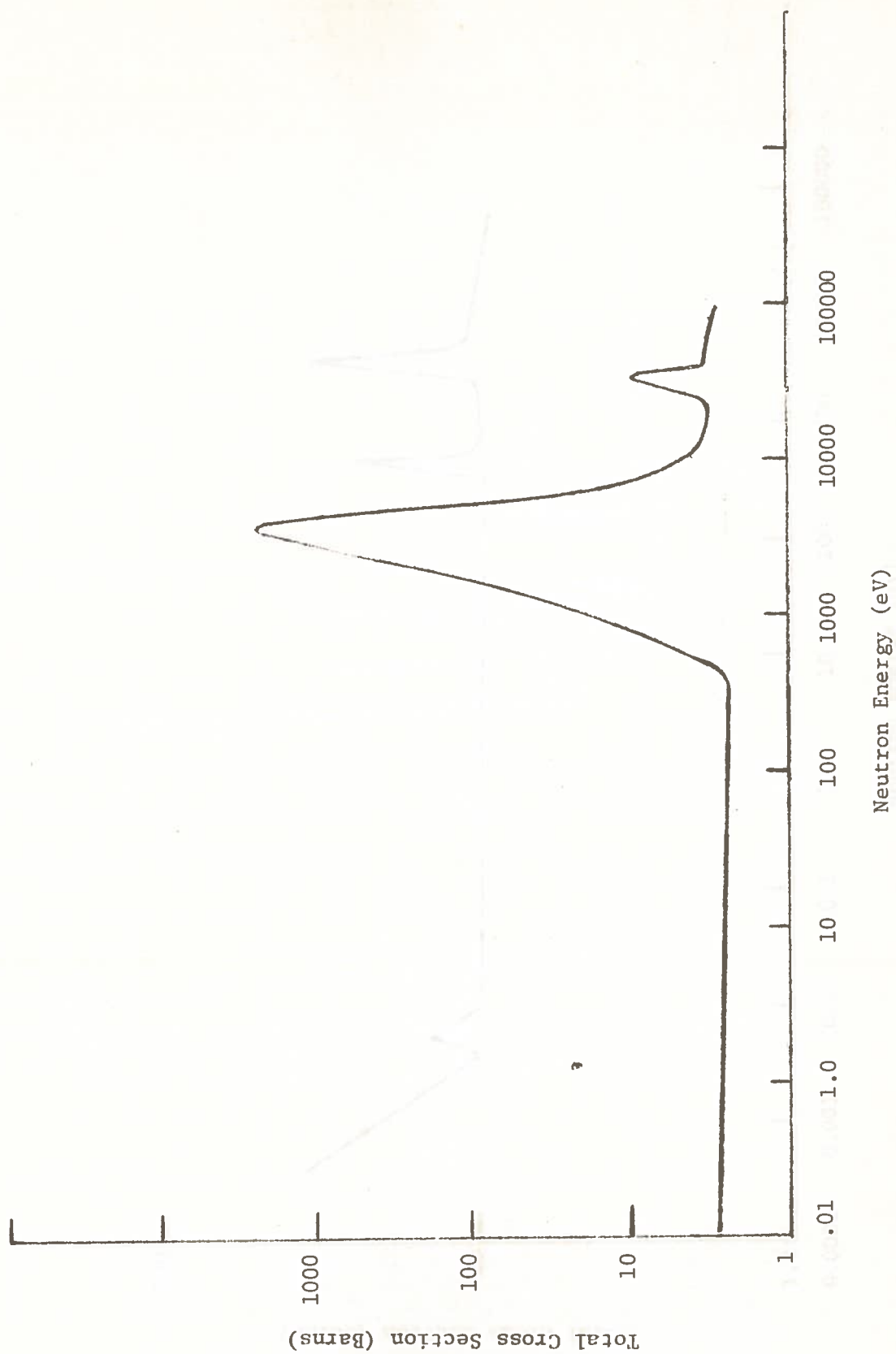


FIGURE 5. Total Cross Section Versus Neutron Energy for Na-23

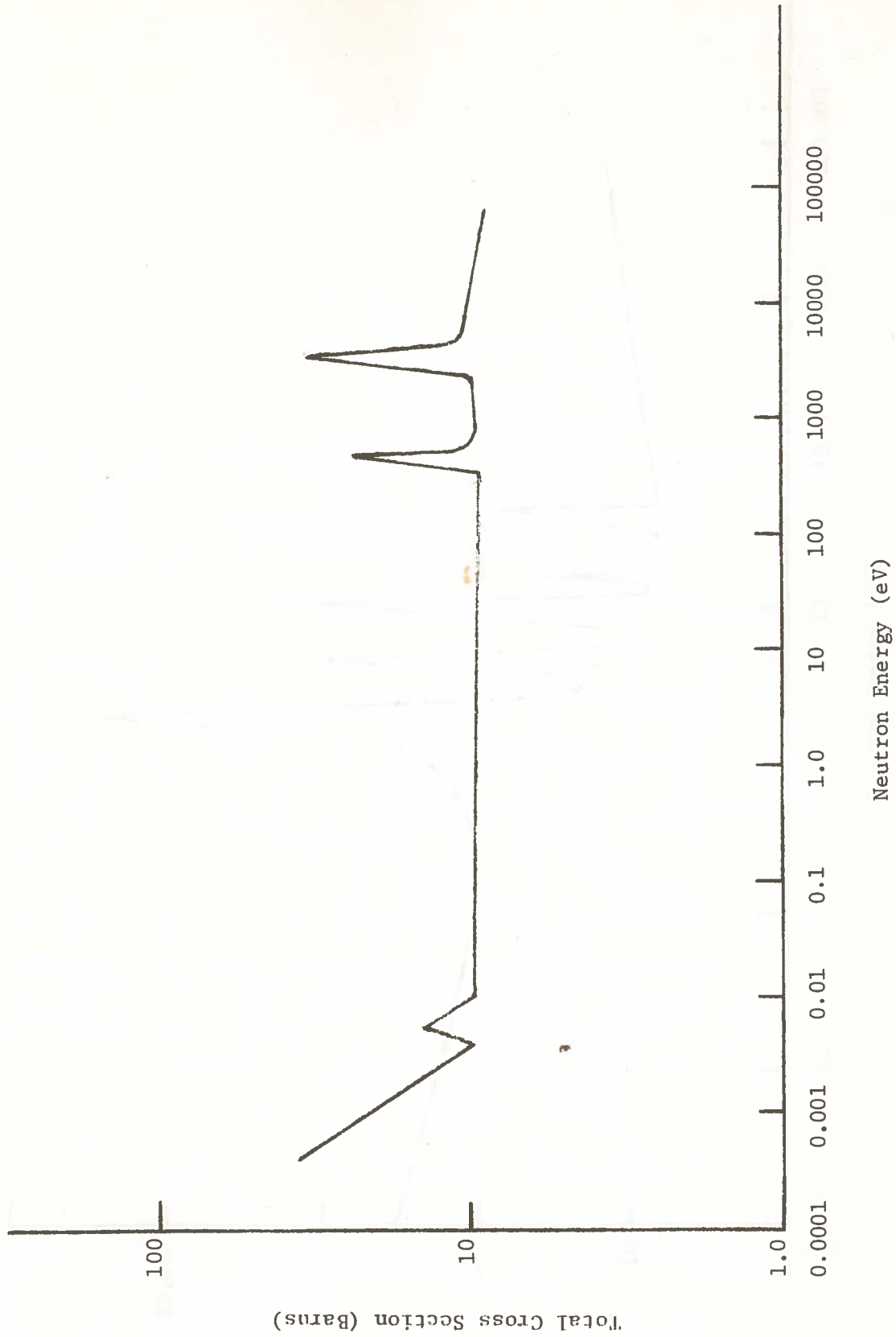


FIGURE 6. Total Cross Section Versus Neutron Energy for Cu-63



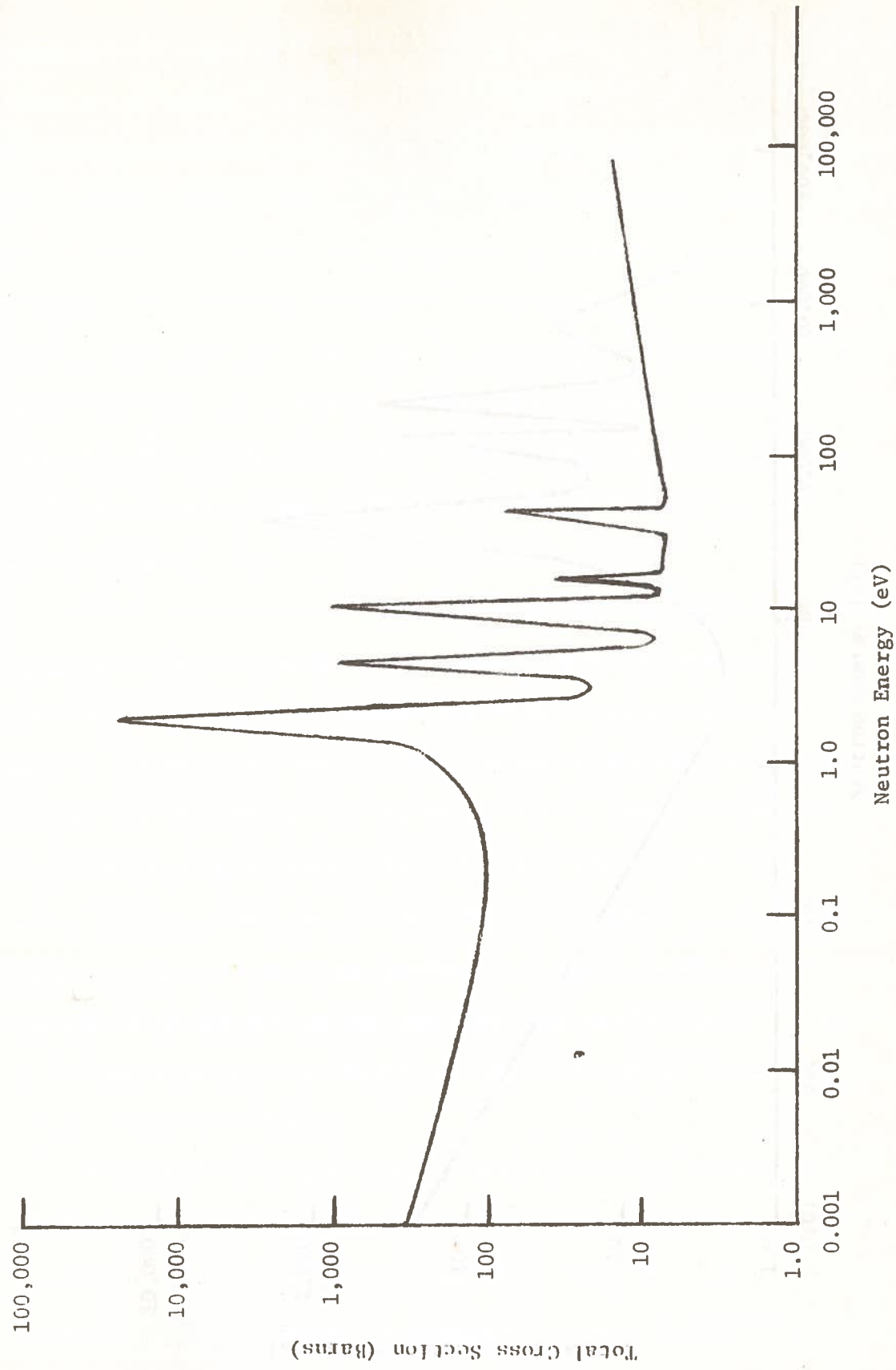


FIGURE 7. Total Cross Section Versus Neutron Energy for In-115

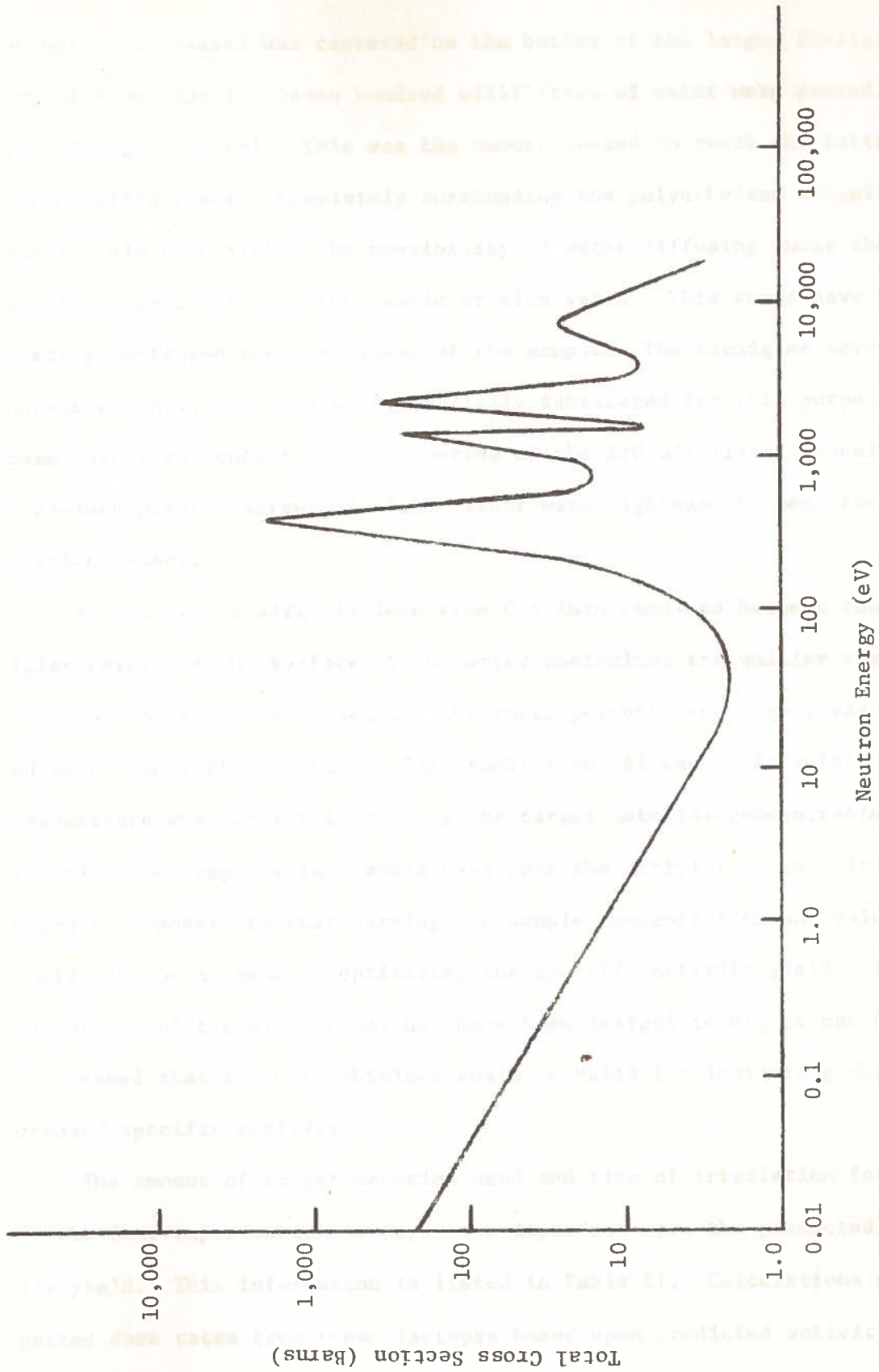


FIGURE 8. Total Cross Section Versus Neutron Energy for Mn-55

polyethylene vessel was centered on the bottom of the larger Plexiglas irradiation vessel. Seven hundred milliliters of water were poured into the Plexiglas vessel. This was the amount needed to reach the bottom of the paraffin cover. Completely surrounding the polyethylene vessel with water would have risked the possibility of water diffusing under the paraffin cover and into the sample or vice versa. This would have completely destroyed the usefulness of the sample. The Plexiglas cover was depressed until the moderator, specially fabricated for this purpose, came into firm contact with the bottom of the 120 milliliter vessel. The 0.25-inch plastic screw and fiber washer were tightened to seal the irradiation vessel.

An air gap of slightly less than 0.5-inch remained between the Plexiglas cover and the surface of the water encircling the smaller vessel. This had to be tolerated because the small polyethylene vessel was designed as a temporary structure. This smaller vessel was built solely to demonstrate what effect increasing the target material concentration by reducing the sample volume would have upon the activity yield. It was hoped to demonstrate that varying the sample concentration and volume could also be a means of optimizing the specific activity yield. Although the effect of the air gap may not have been insignificant, it can be safely assumed that the data obtained would be valid for indicating the increased specific activity.

The amount of target material used and time of irradiation for each of the four experimental isotopes was dependent upon the predicted activity yield. This information is listed in Table II. Calculations of expected dose rates from these isotopes based upon predicted activity yields are shown in Appendix B.

TABLE II  
 QUANTITIES OF TARGET ISOTOPES AND IRRADIATION TIMES USED  
 FOR EXPERIMENTAL MEASUREMENTS

RADIOISOTOPE	HALF LIFE	IRRADIATION TIME (HOURS)	WEIGHT OF TARGET ISOTOPE (gm)
Na-24	15 h	2.0	9.0
Cu-64	12.75 h	2.0	4.5
In-116m	54.1 m	0.5	0.045
Mn-56	2.58 h	0.5	0.45

Activation Procedure. All activations were performed in the Louisiana State University Californium-252 Demonstration Center tank. This tank is the principle storage facility for californium-252 sources which were made available to the university by the Atomic Energy Commission. It is 4 feet wide, 8 feet long, 6.5 feet high and is constructed of stainless steel plate. The tank is filled with water and shielded on three sides and the bottom by concrete blocks packed with borated sand. The source storage configuration in the tank is illustrated in Figure 9. All californium-252 sources except for the 10 milligram source are in the source holder nearer to one end of the tank during activation. This allows the other end of the tank to be used for activation without interference from other sources. For all practical purposes, it can be assumed that no neutrons from sources other than the 10 milligram source used for activation reach the irradiation vessel.

For all activations the irradiation vessel was lowered onto a Plexiglas stand located approximately 1.5 feet from the sides of the tank as shown in Figure 9. The stand supported the irradiation vessel in a level position approximately one foot from the bottom of the tank. The Plexiglas wall of the irradiation vessel and the water surrounding the vessel serve as a neutron reflecting medium. This has the effect of increasing the average neutron flux over the entire volume of the vessel. Keeping the vessel supported in this manner prevented the tank walls and bottom from perturbing the neutron flux in and immediately around the volume of the vessel.

To begin activation, the 10 milligram californium-252 source was quickly moved from its storage position and inserted into the center of



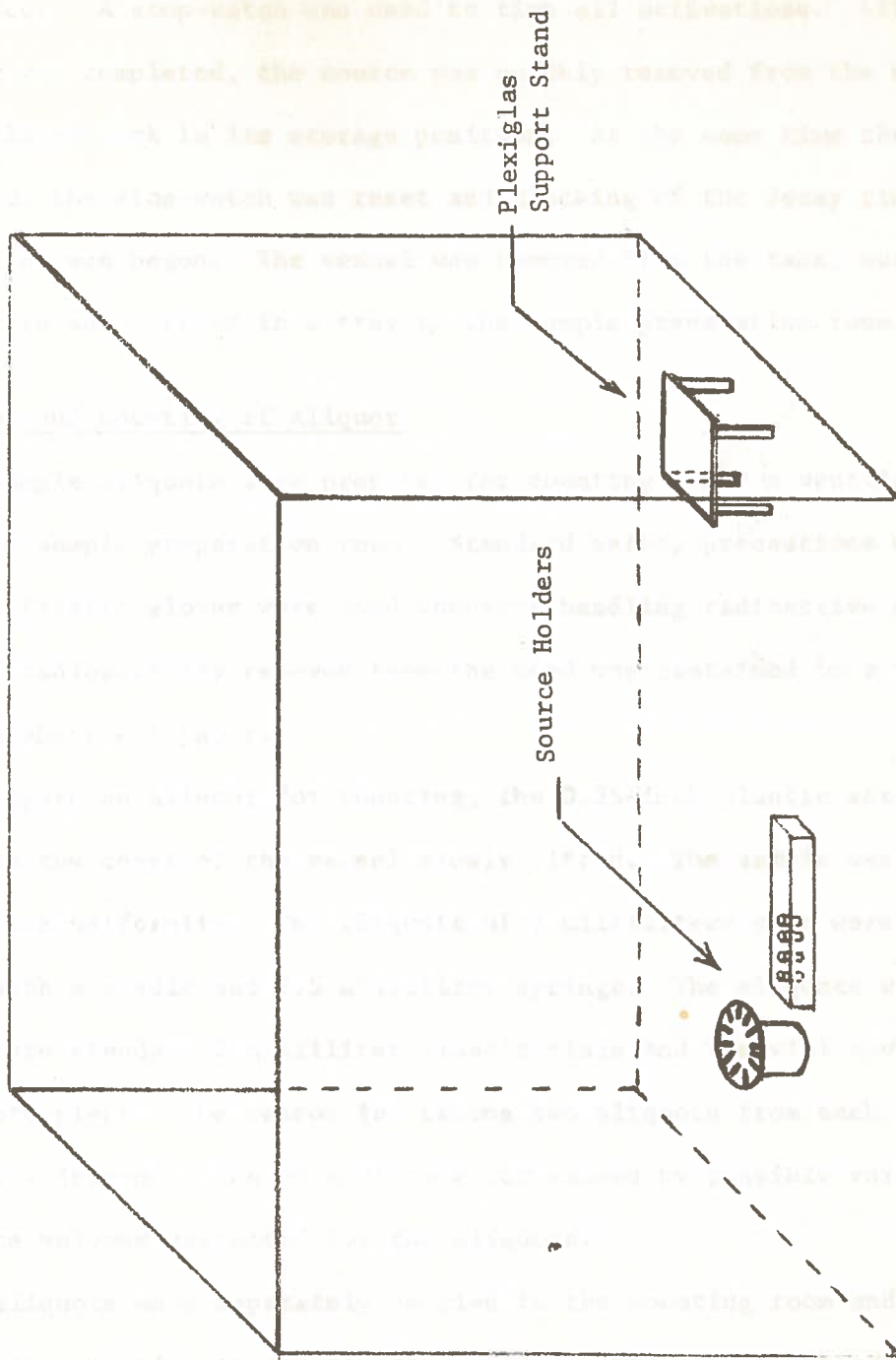


FIGURE 9. Water Tank Storage and Activation Facility for Cf-252 Sources

the moderator. A stop-watch was used to time all activations. After activation was completed, the source was quickly removed from the moderator and placed back in its storage position. At the same time the source was removed, the stop-watch was reset and clocking of the decay time before counting was begun. The vessel was removed from the tank, surveyed for dose rate and carried in a tray to the sample preparation room.

#### Preparation and Counting of Aliquot

All sample aliquots were prepared for counting under a ventilation hood in the sample preparation room. Standard safety precautions were followed. Plastic gloves were used whenever handling radioactive material. All radioactivity removed from the hood was contained in a tray lined with absorbent paper.

To prepare an aliquot for counting, the 0.25-inch plastic screw was removed and the cover of the vessel slowly lifted. The sample was stirred to assure uniformity. Two aliquots of 2 milliliters each were taken randomly with a needle and 2.5 milliliter syringe. The aliquots were injected into standard 2 milliliter plastic vials and the vial covers snapped into place. The reason for taking two aliquots from each sample was to allow determination of maximum error caused by possible variations between the volumes extracted for the aliquots.

The aliquots were separately carried to the counting room and placed into counting position in the counting shield. The top of the counting shield was closed. Decay times were recorded and each aliquot was counted for four minutes. The detection system had been calibrated and a four minute background count taken prior to the counting of the aliquots.

After counting, the aliquots were labeled with the radioisotope and their approximate activity and placed in a shield at the rear of the hood. The front and sides of the hood were surveyed and the dose rates posted at the front of the hood.

Before preparing another sample, the irradiation vessel was emptied and decontaminated. The radioactive sample was stored in a one liter polyethylene bottle. Paper Kim-wipes\* were used to remove most of the contamination. The small amount of contamination remaining on the vessel parts was removed by flushing with "radiac-wash" and water.

#### Counting Equipment and Geometry

The counting system used for aliquot counting is shown schematically in Figure 10. This equipment allowed fast and simple determination of aliquot activities by standard gamma spectroscopy.

For reproduction of counting geometry, a Plexiglas stand-off was built and used for sample counting. The stand-off, shown in Figure 11, was constructed using 0.187-inch Plexiglas rods and 0.125-inch thick, rectangular Plexiglas plates. They were cemented together with Plexiglas cement. A 0.50-inch hole was drilled at the center of the top plate. This was to allow the 0.5-inch diameter plastic vial containing an aliquot from the sample to be positioned for counting. The dimensions used allow the 2 milliliter aliquot to be counted in a shielded, fixed position with its geometrical center 10 centimeters above the center of the NaI(Tl) crystal surface. In this configuration the aliquot approximates a point source of radiation.

\* Trademark of Kimberly-Clark Corporation.

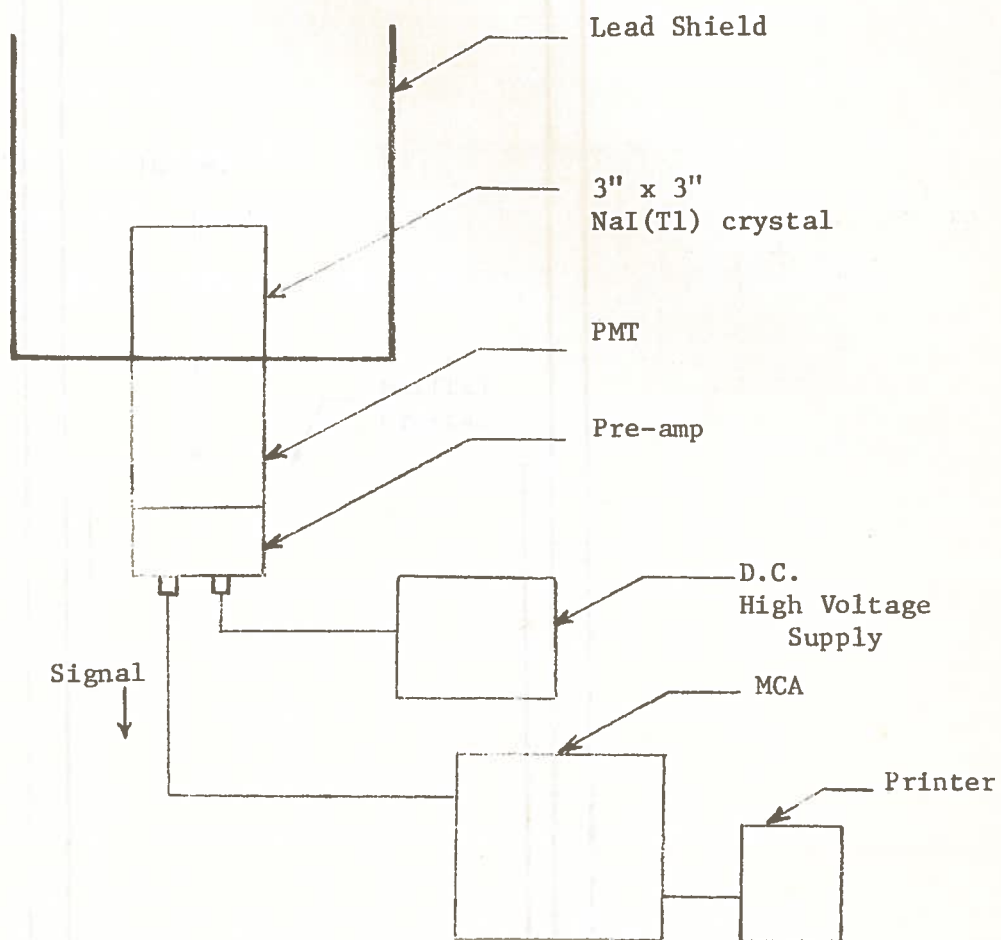


FIGURE 10. Schematic of Counting System

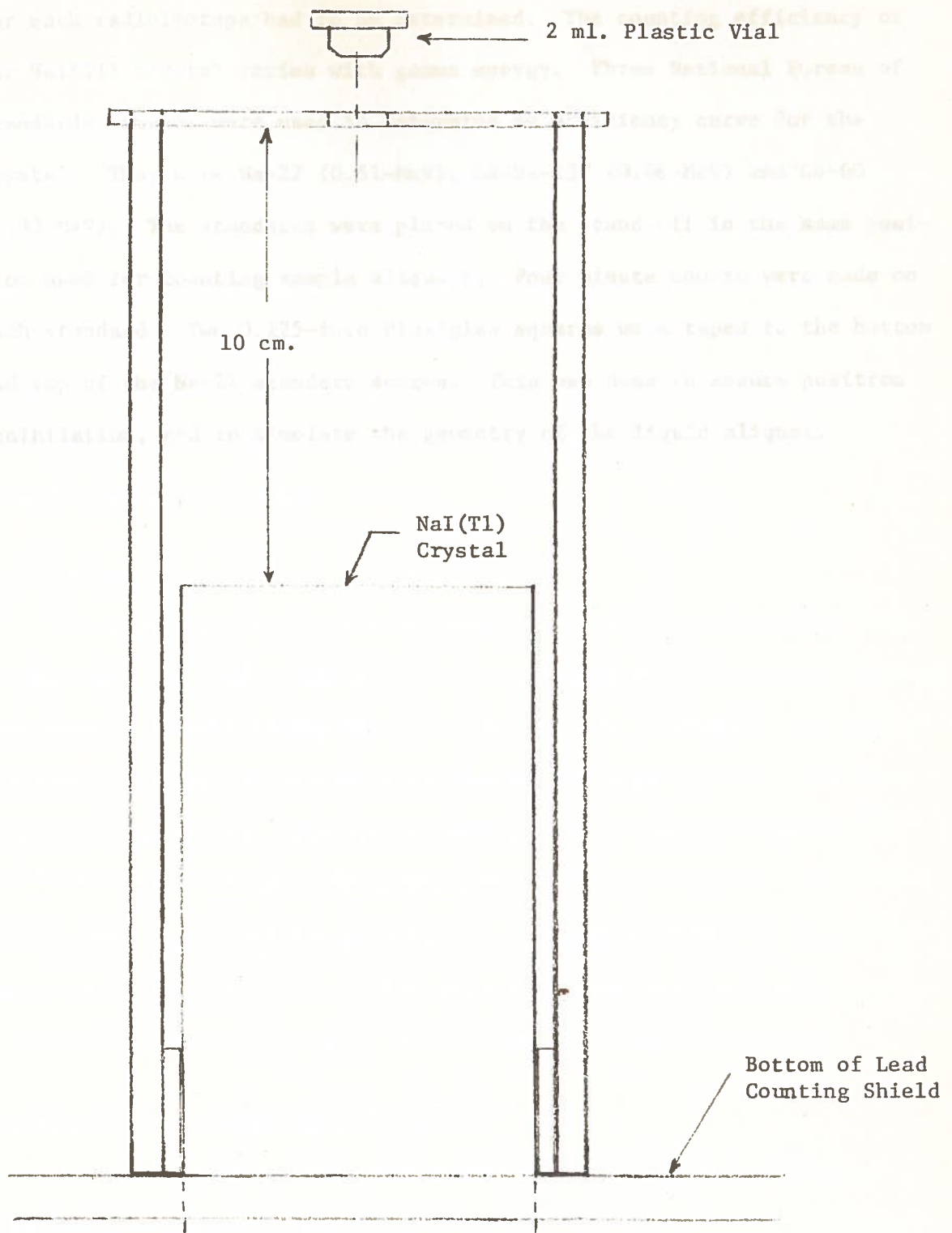


FIGURE 11. Plexiglas Stand-off for Aliquot Counting



To obtain the experimental activity yields, the counting efficiency for each radioisotope had to be determined. The counting efficiency of the NaI(Tl) crystal varies with gamma energy. Three National Bureau of Standards sources were used to determine an efficiency curve for the crystal. They were Na-22 (0.51-MeV), Cs-Ba-137 (0.66-MeV) and Co-60 (1.33-MeV). The standards were placed on the stand-off in the same position used for counting sample aliquots. Four minute counts were made on each standard. Two 0.125-inch Plexiglas squares were taped to the bottom and top of the Na-22 standard source. This was done to assure positron annihilation, and to simulate the geometry of the liquid aliquot.

#### Calculation of Experimental Activity Yields

The experimental activity yields were calculated using equation (2-12). Values used for  $Z$  were number of nuclei per gram of stable target isotope. For example in calculating the activity yield for sodium-24, one gram of sodium-23 was used to determine the number of target nuclei. The cross sections used are for neutrons at 205 meters per second velocity. (12)

The data corrected in accordance with equation (2-8). Activation yields were determined for irradiation times of one hour, 12 hours, one day, seven days and 10 days. The corrected cross sections and activation yields are tabulated in Table III for each selected radioisotope.

#### Interrelation of Counting Efficiency

The efficiency of detection using the total-peak-area method for each of the four experimental radioisotopes is shown in Table IV. These were obtained by interpolation from the experimental detection efficiency

## CHAPTER IV

### CALCULATED AND EXPERIMENTAL RESULTS

#### Californium-252 Thermal Flux Distribution

The thermal neutron flux distribution for a 10 milligram californium source in water is shown in Figure 12. This data was obtained from ANISN and DOT code calculations, and is listed in Appendix C. From the DOT calculations the thermal neutron flux at the surface of this source was determined to be approximately  $10^8$  neutrons  $\text{cm}^{-2}\text{-sec}^{-1}$ . This value was used in all calculations of predicted activity yields for the various radioisotopes of interest.

#### Calculation of Theoretical Activity Yields

All calculations of activity yields were made using equation (2-12). Values used for N were number of nuclei per gram of stable target isotope. For example in calculating the activity yield for sodium-24, one gram of sodium-23 was used to determine the number of target nuclei. The cross sections used are for neutrons at 2200 meters per second velocity. <sup>(12)</sup>, <sup>(13)</sup> They were corrected in accordance with equation (2-8). Activation yields were determined for irradiation times of one hour, 12 hours, one day, seven days and 30 days. The corrected cross sections and activation yields are tabulated in Table III for each selected radioisotope.

#### Determination of Counting Efficiency

The efficiency of detection using the total-peak-area method for each of the four experimental radioisotopes is shown in Table IV. These were obtained by interpolation from the experimental detection efficiency

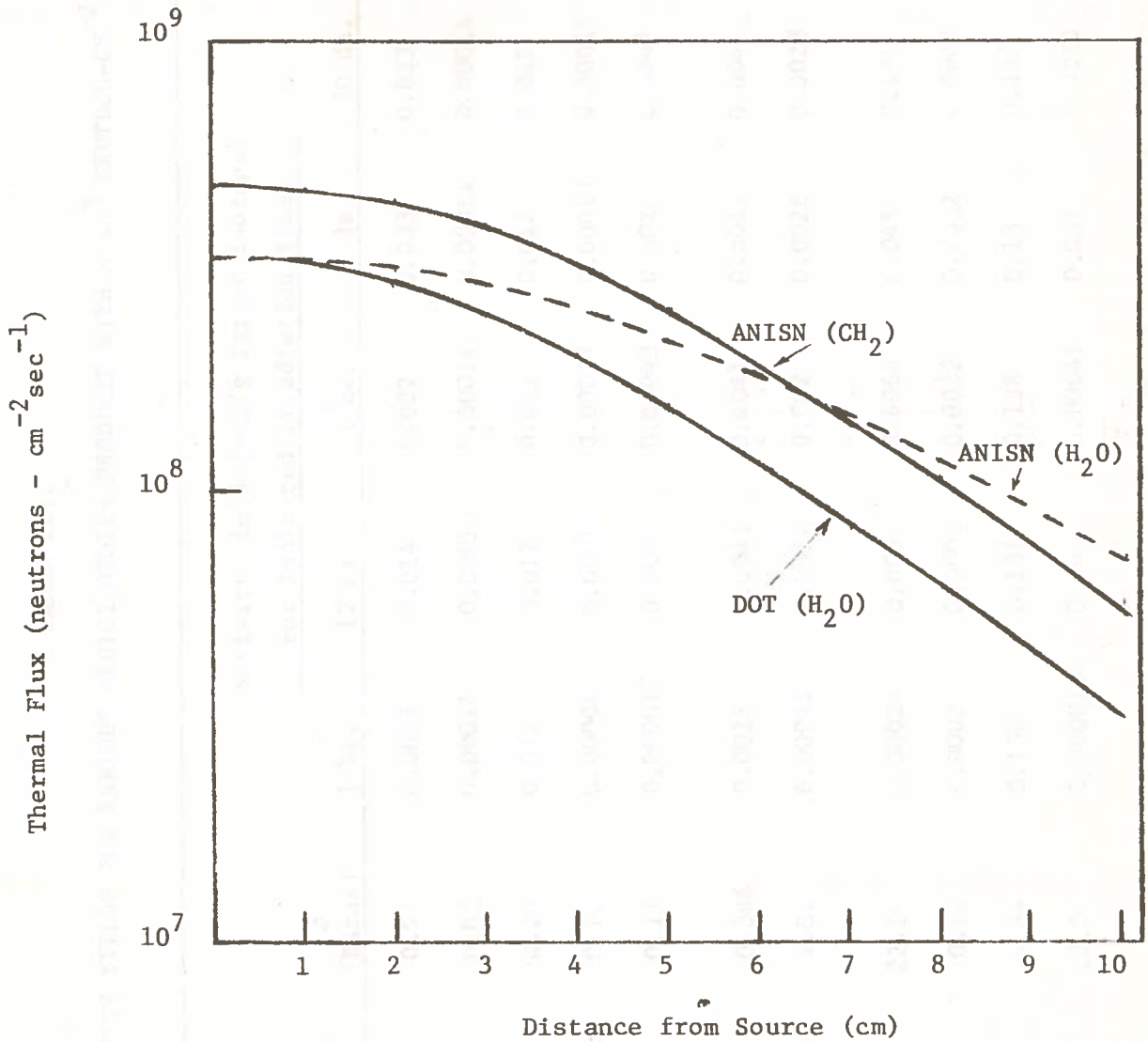


FIGURE 12. Thermal Flux Distribution Obtained from ANISN and DOT Code Calculations

TABLE III.  
 CALCULATED ACTIVITY YIELDS FOR VARIOUS RADIOISOTOPES PRODUCED WITH A  $10^8$  NEUTRON-CM<sup>-2</sup> SEC<sup>-1</sup> FLUX

Radioisotope	Half Life	$\bar{\sigma}$ (Barns)	Activity Yield (mci/g Target Isotope) For Indicated Irradiation Times				Some Medical Applications	
			1 hr.	12 hr.	1 da.	7 da.		30 da.
Na-24	15. hr	0.47	0.0015	0.014	0.022	0.033	0.033	Sodium Space
Mg-27	9.5m	0.02	0.00014	0.00014	0.00014	0.00014	0.00014	
Al-28	2.27m	0.20	0.012	0.012	0.012	0.012	0.012	
Si-31	2.62hr	0.10	0.00004	0.00016	0.00017	0.00017	0.00017	Lung Cancer Therapy
P-32	14.3da	0.17	0.000017	0.0002	0.00043	0.0026	0.0069	
Cl-38	37.2m	0.386	0.0027	0.0041	0.0041	0.0041	0.0041	
K-42	12.4hr	1.02	0.00015	0.0017	0.002	0.0028	0.0028	Electrolyte Space
Sc-46	83.8da	22.16	0.00024	0.003	0.0064	0.045	0.176	
Ti-51	5.76m	0.12	0.0002	0.0002	0.0002	0.0002	0.0002	
V-52	3.75m	4.34	0.130	0.138	0.138	0.138	0.138	
Cr-51	27.8d	12.0	0.000016	0.0002	0.00041	0.0027	0.0089	Spleen Scanning, Red Cell Survival





Br-82	35.4hr	3.1	0.0006	0.0065	0.011	0.029	0.031	Bladder Scanning & Bladder Tumor Therapy
Rb-86	18.66da	0.64	<10 <sup>-5</sup>	0.00016	0.0003	0.002	0.006	Muscular Dystrophy; Myocardium Scanning
Sr-87 <sup>m</sup>	2.83hr	1.2	0.0005	0.0021	0.0022	0.0022	0.0022	Bone Scanning; Metabolism
Y-90 <sup>m</sup>	64.hr	1.1	0.000014	0.00017	0.0003	0.0012	0.0014	Intrapulmonary Applications
Nb-94	6.26m	0.9	0.0157	0.0158	0.0158	0.0158	0.0158	
Mo-99	66.6hr	0.4	0.000015	0.0002	0.00035	0.0013	0.0016	Yields Tc-99 <sup>m</sup> T 1/2 = 6 hr. Brain Scanning, Aerosol Lung Scanning
Mo-101	14.6m	0.18	0.00026	0.00028	0.00028	0.00028	0.00028	
Ru-105	4.44hr	0.6	0.00025	0.0015	0.0017	0.00175	0.00175	
Rh-104	4.36m	10.6	0.168	0.168	0.168	0.168	0.168	
Pd-103	17.da	4.3	<10 <sup>-5</sup>	0.000013	0.000026	0.00016	0.00047	
Pd-109	4.69m	0.17	0.00068	0.00068	0.00068	0.00068	0.00068	
Pd-111	22.m	0.27	0.0004	0.00047	0.00047	0.00047	0.00047	
Ag-108	2.42m	39.0	0.307	0.307	0.307	0.307	0.307	Scanning; Dynamic Studies

Cd-107	6.5h	0.9	0.00002	0.00012	0.00016	0.00017	0.00017	
Cd-111	48.6m	0.2	0.00021	0.00036	0.00036	0.00036	0.00036	
Cd-117	2.5hr	1.3	0.00034	0.00135	0.0014	0.0014	0.0014	
In-114	71.9sec	1.9	0.0012	0.0012	0.0012	0.0012	0.0012	Dynamic Studies
In-116 <sup>m</sup>	54.1m	129.0	0.937	1.75	1.75	1.75	1.75	Bone Scanning; Brain Scanning; Perfusion Studies
Sn-121	26.2hr	0.12	0.000014	0.00015	0.00025	0.00053	0.00053	
Sn-123	40.3m	0.14	0.00006	0.00009	0.00009	0.00009	0.00009	
Sn-125	9.6m	0.18	0.00013	0.00013	0.00013	0.00013	0.00013	
Sb-122	2.74da	6.0	0.00046	0.0055	0.011	0.038	0.046	
Te-127	9.3hr	0.7	0.00012	0.001	0.0014	0.0017	0.0017	
Te-129	69.m	0.12	0.00023	0.0005	0.0005	0.0005	0.0005	
Ie-131	25.m	0.2	0.00015	0.00018	0.00018	0.00018	0.00018	
I-128	25.m	4.9	0.050	0.062	0.062	0.062	0.062	I-3 Test Plasma Volume; Kidney Function; Thyroid; Lung Scanning
Cs-134 <sup>m</sup>	2.9hr	0.015	0.00004	0.00017	0.00018	0.00018	0.00018	
Ba-135 <sup>m</sup>	28.7hr	2.0	0.000013	0.00016	0.00025	0.00057	0.00058	Bone Scanning
Ba-137 <sup>m</sup>	2.55m	0.4	0.00037	0.00037	0.00037	0.00037	0.00037	
Ba-139	83.2m	0.44	0.00145	0.0037	0.0037	0.0037	0.0037	Bone Scanning

La-140	40.2hr	7.7	0.0015	0.016	0.029	0.0817	0.0866
Ce-137	9.hr	5.6	$<10^{-5}$	0.00008	0.00011	0.00013	0.00013
Ce-141	32.5da	0.27	$<10^{-5}$	0.00003	0.00006	0.00038	0.0013
Pr-142	14.6m	3.5	0.037	0.04	0.04	0.04	0.04
Pr-142	19.2h	8.9	0.0035	0.0358	0.059	0.102	0.102
Nd-147	11.06da	1.6	$<10^{-5}$	0.000095	0.00019	0.0011	0.0026
Nd-149	1.73hr	3.3	0.00066	0.002	0.002	0.002	0.002
Nd-151	12.4m	2.5	0.00144	0.0015	0.0015	0.0015	0.0015
Sm-153	46.8hr	124.0	0.005	0.057	0.106	0.325	0.355
Sm-155	22.3m	4.9	0.010	0.0116	0.0116	0.0116	0.0116
Eu-152	96.m	4.0	0.007	0.0198	0.02	0.02	0.02
Eu-152	9.3hr	1241.0	0.454	3.781	5.355	6.398	6.398
Gd-159	18.hr	3.5	0.00033	0.0033	0.0054	0.0089	0.0089
Dy-165	2.35hr	1862.0	1.328	5.052	5.209	5.209	5.209
Ho-166	26.8hr	53.0	0.013	0.139	0.242	0.516	0.523
Er-163	75.m	16.8	0.000097	0.00023	0.00023	0.00023	0.00023
Er-169	9.3da	1.8	0.000014	0.00017	0.00033	0.0019	0.0042
Er-171	7.5hr	8.0	0.001	0.0076	0.010	0.0114	0.0114
Yb-169	31.da	11,000.0	0.00013	0.0016	0.0032	0.021	0.0702

Bone Scanning

Bone Scanning

Bone Scanning

Bone Scanning

Yb-175	4.19da	53.0	0.00095	0.0124	0.024	0.108	0.1564	Bone Scanning
Yb-177	1.9hr	4.9	0.0017	0.0056	0.0057	0.0057	0.0057	Bone Scanning
Lu-176 <sup>m</sup>	3.7hr	31.0	0.048	0.251	0.277	0.2809	0.2809	Bone Scanning
Lu-177	6.7da	3,540.0	0.0034	0.042	0.083	0.437	0.773	Bone Scanning
Hf-180 <sup>m</sup>	5.5hr	57.6	0.0085	0.056	0.068	0.072	0.072	Bone Scanning
Hf-181	42.4da	8.9	0.000017	0.00023	0.00045	0.003	0.011	Bone Scanning
Ta-182	15.9m	0.03	0.00025	0.00026	0.00027	0.00027	0.00027	Bone Scanning
W-187	23.9hr	30.0	0.0021	0.0218	0.0374	0.0740	0.0746	Bone Scanning
Re-186	91.hr	88.6	0.002	0.025	0.0483	0.208	0.2875	Bone Scanning
Os-189 <sup>m</sup>	5.9hr	3.80 <sup>(12)</sup>	0.0005	0.0033	0.0041	0.0044	0.0044	Bone Scanning
Os-191	13.hr	8.07 <sup>(12)</sup>	0.00095	0.0086	0.013	0.0182	0.0183	Bone Scanning
Os-191	15.5da	7.1	0.000029	0.00035	0.0007	0.0043	0.0119	Bone Scanning
Os-193	31.hr	1.4	0.0001	0.0011	0.002	0.0048	0.00486	Bone Scanning
Ir-192	74.3da	621.0	0.00075	0.0091	0.018	0.124	0.481	Bone Scanning
Ir-194	17.8hr	115.2	0.024	0.141	0.375	0.608	0.609	Bone Scanning
Pt-195 <sup>m</sup>	4.1da	1.1	0.00002	0.00024	0.00047	0.0021	0.003	Bone Scanning
Pt-197	20.hr	70.9	0.005	0.051	0.084	0.1485	0.149	Bone Scanning
Pt-199	31.m	3.5	0.0015	0.002	0.002	0.002	0.002	Bone Scanning
Au-198	2.69da	85.1	0.007	0.084	0.159	0.587	0.703	Bone Scanning

Liver Function;  
Aerosol Lung  
Scanning

Hg-197	23.8hr	115.0	0.000004	0.00041	0.0007	0.00138	0.00139	Kidney Function
Hg-197	64.1hr	2750.0	0.00033	0.0004	0.00076	0.028	0.033	Kidney Function
Hg-202	46.6da	3.4	<10 <sup>-5</sup>	0.00006	0.00012	0.0008	0.003	Kidney Function



curve shown in Figure 13. The efficiency curve for a three inch by three inch NaI(Tl) crystal and point sources located 10 centimeters from the surface of the crystal is plotted for comparison. <sup>(14)</sup>

The experimental efficiency calculated for Cu-64 using the Na-22 standard was not consistent with the calculations obtained for the other two standard sources. Recounting and recalculating yielded the same value. This data point was therefore excluded. The Cs-Ba-137 and Co-60 experimental efficiencies were used to construct the experimental efficiency curve. Neglecting the Na-22 efficiency determination, the experimental results are very similar to those obtained from Heath. <sup>(14)</sup> The method of calculation used is shown in Appendix D.

TABLE IV. EXPERIMENTAL EFFICIENCIES

<u>Radioisotope</u>	<u>E (MeV)</u>	<u>Peak Efficiency</u>
Cu-64	0.51	0.0124
Mn-56	0.84	0.0077
In-116m	1.29	0.00522
Na-24	1.39	0.00493

#### Experimental Activity Yields

Activity yields of the experimental radioisotopes were determined for each increment of moderator thickness. These are saturated activity yields calculated on the basis of activity yields obtained for the irradiation times used during experimentation. The method of calculating

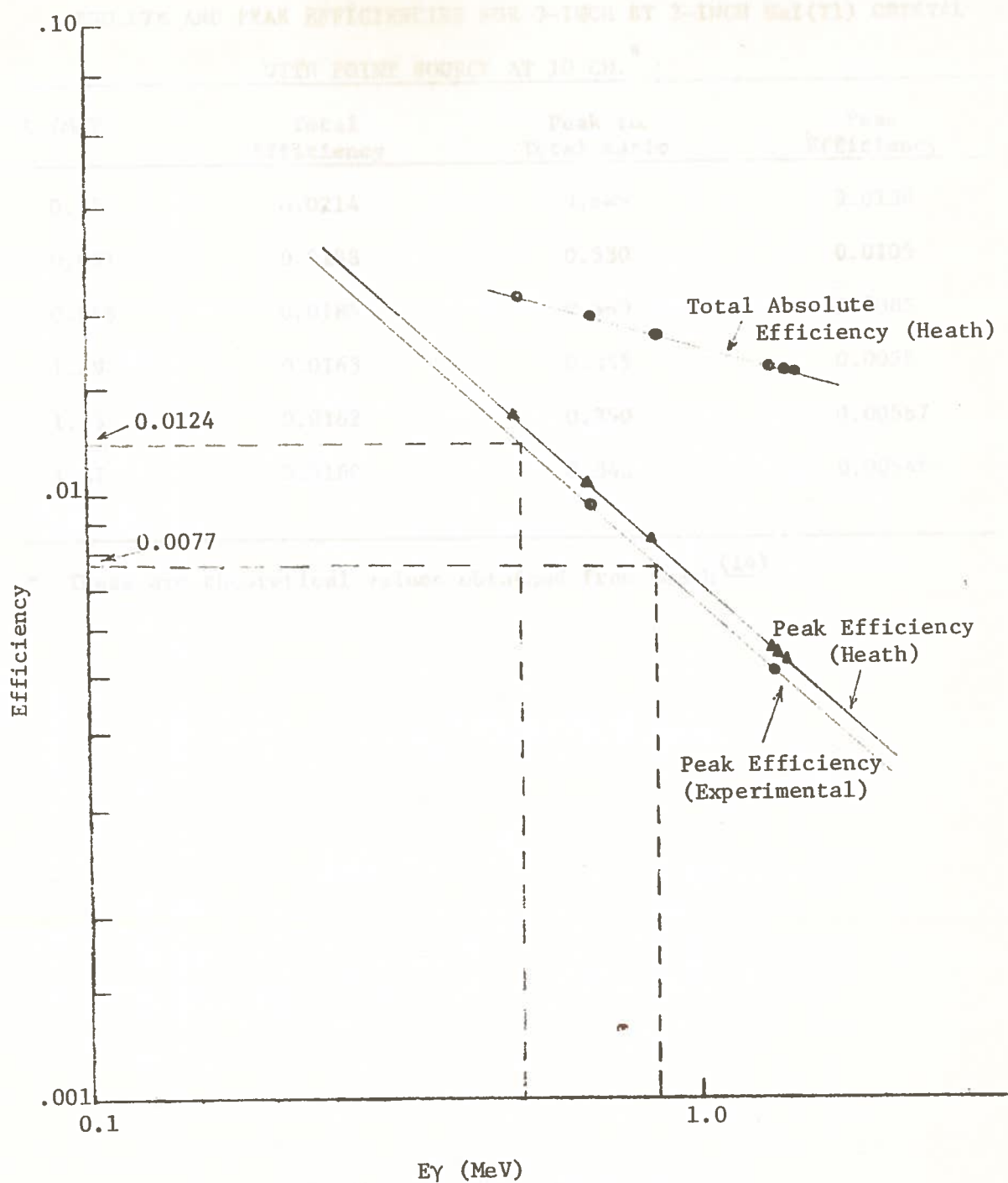


FIGURE 13. A Comparison of Theoretical and Experimental Peak Efficiencies for a 3 Inch by 3 Inch NaI(Tl) Crystal with Point Source at 10 cm.

TABLE V  
 ABSOLUTE AND PEAK EFFICIENCIES FOR 3-INCH BY 3-INCH NaI(Tl) CRYSTAL  
 WITH POINT SOURCE AT 10 CM.\*

E (MeV)	Total Efficiency	Peak to Total Ratio	Peak Efficiency
0.51	0.0214	0.645	0.0138
0.661	0.0198	0.530	0.0105
0.846	0.0185	0.460	0.0085
1.29	0.0163	0.355	0.0058
1.33	0.0162	0.350	0.00567
1.37	0.0160	0.343	0.00548

\* These are theoretical values obtained from Heath <sup>(14)</sup>.

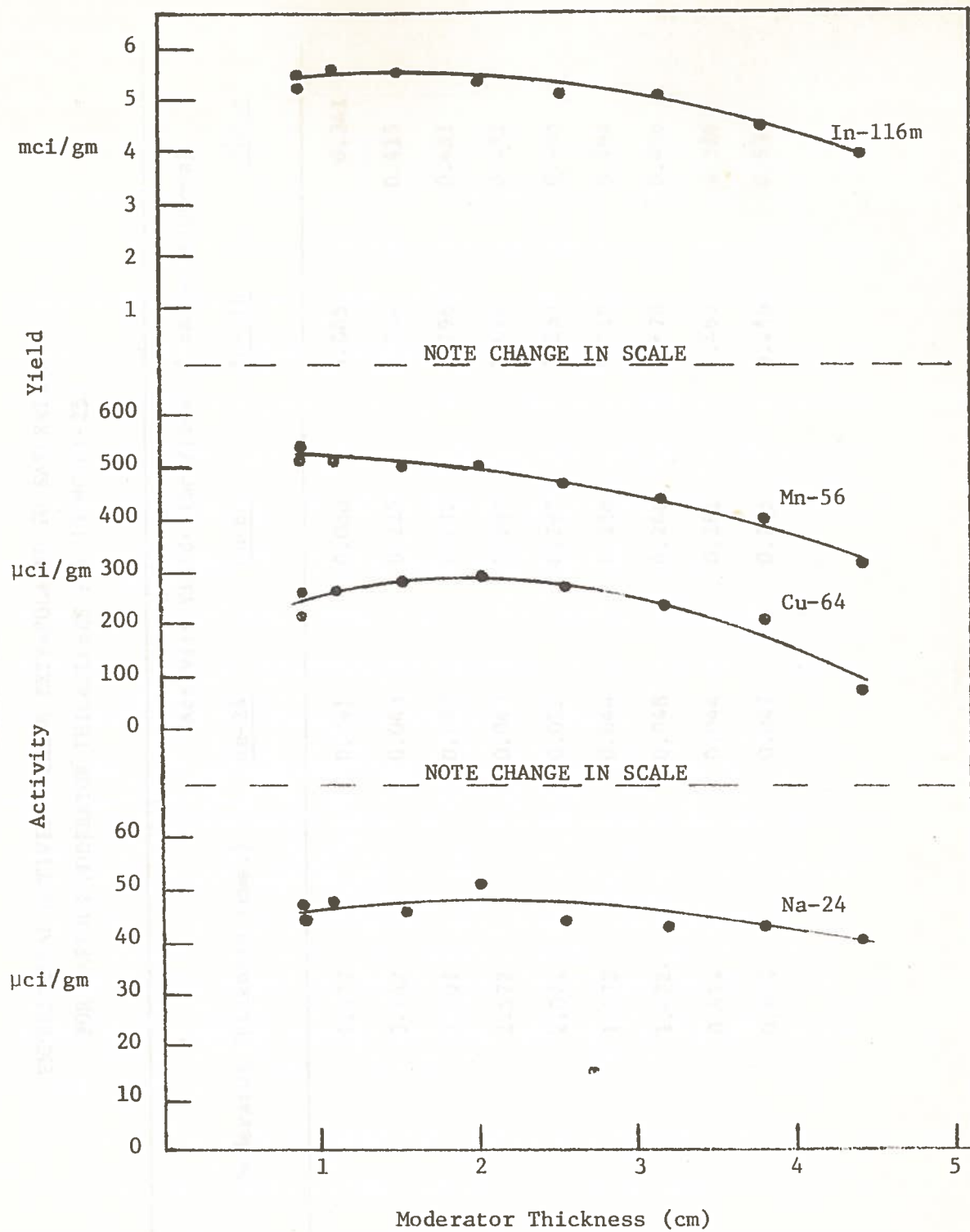


FIGURE 14. Saturated Activity Yield Versus Moderator Thickness

TABLE VI.

EXPERIMENTAL ACTIVITY YIELDS EXTRAPOLATED TO SATURATION  
FOR VARIOUS MODERATOR THICKNESSES FOR 10 MG CF-252

Sample	Moderator Thickness (cms.)	Activity Yields (mci/gram of target isotope)			
		<u>Na-24</u>	<u>Cu-64</u>	<u>In-116</u>	<u>Mn-56</u>
1	4.477	0.041	0.080	4.005	0.341
2	3.842	0.043	0.225	4.546	0.415
3	3.207	0.042	0.232	5.196	0.451
4	2.572	0.043	0.267	5.072	0.472
5	2.072	0.051	0.297	5.259	0.495
6	1.572	0.044	0.288	5.519	0.494
7	1.072	0.048	0.266	5.670	0.496
8	0.914	0.044	0.261	5.465	0.516
9	0.914	0.047	0.205	5.246	0.534



these yields is given in Appendix D. The saturation activity yields as a function of moderator thickness are plotted in Figure 14.

From Figure 14 it is seen that the moderator thickness of two centimeters is close to optimum for the sodium-24 and copper-64 radioisotopes. That is, for these two isotopes the activation yield appears to peak at two centimeters and begins to fall off as the moderator is further reduced. This reduction is probably caused by the increase in average energy of the neutron flux in the sample region near the moderator. This increase in average energy is a result of the reduction in moderator thickness. It could also be partially caused by the increase in radial thickness of the sample as the moderator is reduced. The outer portion of the sample is in effect seeing a neutron flux that has passed through an absorbing medium which is increasing in radial thickness each time the moderator radius is reduced.

The optimum moderator thickness for indium-116m is, refer to Figure 14, approximately one centimeter. This appears to be the thickness which allows the maximum use of the 1.5 eV resonance absorption peak. The decrease in activity yield for moderator thickness less than one centimeter may be caused by the increase in average energy of the flux combined with reducing effect caused by increased radial thickness of the sample.

In the case of manganese-56 there was a fairly consistent increase in the activity yield as the moderator thickness was reduced. The increase in radial thickness of the sample caused no noticeable effect. The increasing activity yield is most likely caused by the large resonance absorption in the 300-eV region. For activations of manganese-55 a moderator thickness of one centimeter may be considered optimum.

From Table III the theoretical activation yields for sodium-24, copper-64, indium-116m and manganese-56 are 0.033, 0.063, 1.75 and 0.349 millicuries per gram of target isotope, respectively. These are saturation activities calculated with an assumed thermal flux of  $1.0 \times 10^8$  n-cm<sup>-2</sup>sec<sup>-1</sup>. The maximum experimental yields were 0.051, 0.297, 5.67 and 0.516 respectively. The experimental yields were thus 1.55, 4.7, 3.24 and 1.48 times greater than the theoretical thermal flux yields. The experimental yields for the 120 milliliter indium-116m and manganese-56 samples were 7.436 and 9.577 millicuries per gram. These are saturation activities obtained for 1.072 centimeter thickness of moderator. These values are 1.31 and 1.12 times the 900 milliliter experimental yields, indium-116m and manganese-56.

#### Average Activation Flux

Once the maximum activity yields for each experimental radioisotope have been obtained, equation (2-12) can be used to determine the effective thermal activation flux. This value may be taken as the average activation flux throughout the entire volume of the vessel. This average flux was determined for both the 900 and 120 milliliter samples. The results are shown in Table VII. These values compared quite well with the DOT and ANISN predictions mentioned in CHAPTER II and APPENDIX C.

TABLE VII.  
EFFECTIVE ACTIVATION FLUX DETERMINED FROM  
EXPERIMENTAL ACTIVITY YIELDS

Isotope	Sample Volume (cm)	(n-cm <sup>-2</sup> sec <sup>-1</sup> )
Na-24	900	1.55 x 10 <sup>8</sup>
Cu-64	900	4.7 x 10 <sup>8</sup>
In-116m	900	3.24 x 10 <sup>8</sup>
Mn-56	900	1.48 x 10 <sup>8</sup>
In-116m	120	4.25 x 10 <sup>8</sup>
Mn-56	120	1.65 x 10 <sup>8</sup>

## CHAPTER V

### CONCLUSIONS AND CRITIQUE

From a radiation safety standpoint, both the 900 and 120 milliliter irradiation vessels performed satisfactorily. The vessel design also functioned well mechanically. Although easy to construct, the vessel had two unwanted features. These features were variation in the height and variation in the radial thickness of the sample. The overall height variation was considered to have negligible effect upon the activity yield. There was a slight degree of uncertainty as to the impact that variation in the radial thickness of the sample would have upon the activity yield. The method of adding cylindrical inserts to reduce the radius of the vessel as the moderator is reduced could have been used. This was decided against because of the expense, but perhaps it may have been the only method of avoiding this problem. If this effect upon the activity yield is ignored, general predictions as to the expected behavior for each of the four groups of radioisotopes (refer to CHAPTER III, Selection of Experimental Radioisotopes) can be made.

Sodium-24 representing group I, was seen to have a fairly constant yield throughout the entire range of moderator thickness. The maximum yield occurred at a moderator thickness of approximately 2 centimeters.

Copper-64, representing group II, strongly exhibited its  $1/v$  cross section. That is, the activity yield rose to a maximum at approximately 2 centimeters of moderator and fell off as additional moderator was removed. However, because of the inconsistency noted for the sodium-22 efficiency determination, the magnitude of the activity yields for copper-64 are believed to be a factor of two too high.

From the sodium-24 and copper-64 results, it appears that the optimum moderator thickness for groups I and II is approximately 2 centimeters. It is therefore suspected that the average thermal flux throughout the sample volume was maximized with a moderator thickness of 2 centimeters. At this moderator thickness a value of  $1.5$  to  $2.0 \times 10^8$   $\text{n-cm}^{-2} \text{sec}^{-1}$  could be used to predict activity yields.

Indium-116m demonstrated that the moderator thickness arrangement can be varied to obtain a combination of thermal and resonance absorption which will produce a maximum activity yield. The moderator thickness yielding this maximum activity will be a function of the resonance energy. In general, for group III radioisotopes, a moderator thickness of approximately 1.5 centimeters will produce an average activation flux of around  $3.0 \times 10^8$   $\text{n-cm}^{-2} \text{sec}^{-1}$ .

Manganese-56, representing group IV displayed a fairly consistent increase in activity yield as the moderator thickness was reduced. A moderator thickness of approximately one centimeter can be expected to yield an average activation flux of  $1.5 \times 10^8$   $\text{n-cm}^{-2} \text{sec}^{-1}$ .

The results of the 120 milliliter samples showed that activation yields may be optimized by varying both the target material concentration and the sample volume. Thus for a particular radioisotope, there will exist a certain combination of moderator thickness, target material concentration and the sample volume which will produce the optimum activation yield.

Based upon theoretical activation yields the radioisotopes showing promise for production using californium-252 are listed in Table VIII. They are classified according to the cross section group which they best



TABLE VIII.  
 RADIOISOTOPES SHOWING PROMISE FOR PRODUCTION  
 WITH 10 MILLIGRAMS OF CF-252

Radioisotope	Half Life	Group	Calculated <sup>†</sup> Theoretical Activity	Predicted <sup>††</sup> Activity
Na-24	15h	I	0.033 mci/g	0.051 mci/g *
Sc-46	83.8da	IV	0.17 "	0.255 "
V-52	3.75m	IV	0.138 "	0.207 "
Mn-56	2.58h	IV	0.349 "	0.516 " *
Cu-64	12.75h	II	0.063 "	0.297 " *
Ga-72	14.1h	I	0.04 "	0.06 "
As-76	27h	III	0.08 "	0.24 "
Br-80	17.6m	II	0.078 "	0.117 "
Br-80	4.42h	II	0.027 "	0.405 "
Br-82	35.4h	II	0.031 "	0.0465 "
Nb-94	6.26m	I	0.0158 "	0.0237 "
Rh-104	4.36m	III	0.168 "	0.504 "
Pd-109	13.46h	I	0.042 "	0.063 "
Ag-108	2.42m	III	0.307 "	0.921 "
In-116m	54.1m	III	1.75 "	5.259 " *
Sb-122	2.74da	III	0.046 "	0.138 "
La-140	40.2h	II	0.0866 "	0.130 "
I-128	25m	III	0.062 "	0.186 "
Pr-142	14.6m	III	0.04 "	0.120 "
Pr-142	19.2h	III	0.102 "	0.306 "
Sm-153	46.8h	III	0.355 "	1.065 "

TABLE VIII. (continued)

Eu-152	9.3h	III	6.398	"	19.194	"
Dy-165	2.35h	III	5.209	"	15.627	"
Ho-166	26.8h	III	0.523	"	1.569	"
Yb-175	4.19da	II	0.156	"	0.234	"
Lu-176m	3.7h	III	0.280	"	0.84	"
Lu-177	6.7da	III	0.773	"	2.319	"
Hf-180m	5.5h	III	0.072	"	0.216	"
Re-186	91h	III	0.2875	"	0.8625	"
Ir-192	74.3da	III	0.481	"	1.443	"
Ir-194	17.8h	III	0.609	"	1.827	"
Pt-197	20h	III	0.149	"	0.447	"
Au-198	2.69da	III	0.703	"	2.109	"
Hg-197	64.1h	II	0.033	"	0.495	"

† Activity from thermal flux alone

†† Activity including epithermal flux

\* Based on measured data

resemble. The predicted activity yield based upon the average activation flux is shown for each radioisotope. Medical radioisotopes which show promise for production with 10 milligrams of californium-252 are listed in Table IX.

Other means of increasing the average neutron flux in the irradiation vessel include using a neutron reflector material such as beryllium at the wall of the vessel. Some neutrons which would otherwise escape from the vessel could thus be reflected back. This would further increase the average flux in the system.

The average flux in the vessel could also be increased by positioning sections of enriched uranium fuel rods in a circular arrangement in the center of the source storage tank. Once the irradiation vessel was positioned, neutrons escaping from the vessel would cause fission in the fuel rods. The fuel rods would have to be positioned at a sufficient distance to allow thermalization of the escaped neutrons. This would avoid resonance capture of incoming neutrons by uranium-238. With this arrangement a neutron multiplication effect could be realized. This would increase the average flux in the irradiation vessel.

From the experimental results obtained, it can be concluded that a 10 milligram californium-252 source can definitely be used as a viable means of producing many useful industrial radioisotopes. However, because of the high specific activities required for medical radioisotopes, production with californium-252 will be marginal.

It is hoped that this investigation will prompt additional use of the Louisiana State University Californium-252 Demonstration Center by industrial concerns in the area.

TABLE IX.

MEDICALLY USEFUL RADIOISOTOPES SHOWING PROMISE FOR  
PRODUCTION WITH 10 MILLIGRAMS OF CALIFORNIUM-252

Radioisotope	T <sub>1/2</sub>	Predicted Activity (mci/g Target Isotope)	Possible Medical Applications
Na-24	15.0h	0.051	Sodium Space
Br-80	17.6m	0.156	Bladder Scanning
Ag-108	2.42m	0.921	Scanning; Dynamic Studies
In-116m	54.1m	5.25	Bone Scanning, Brain Scanning, Perfusion Studies
Sm-153	46.8h	1.065	Bone Scanning
Yb-175	4.19da	0.312	" "
Lu-176m	3.7h	0.624	" "
Lu-177	6.7da	2.319	" "
Au-198	2.69da	0.099	Liver Function Aerosol Lung Scanning

## REFERENCES

1. Louis Rosen, "Some Medical Applications of Accelerators", IEEE Transactions on Nuclear Science, vol. 20, (February, 1973), pp. 10 - 23.
2. William A. Jester, et al, "Nuclear Engineering Applications in Medical Science", Isotopes and Radiation Technology, vol. 9, (summer, 1972), pp. 485 - 499.
3. U. S. Atomic Energy Commission, Californium-252 Progress, nos. 1 - 15.
4. K. D. Williams and J. D. Sutton, "Survey of the Uses of Radionuclides in Medicine", Isotopes and Radiation Technology, vol. 6, (summer, 1969), pp. 415 - 424.
5. Standard Research Institute, Survey of the Use of Radionuclides in Medicine, published by U. S. Department of Health, Education and Welfare, Rockville, Maryland, (January, 1970).
6. Arthur R. Foster and Robert L. Wright Jr., Basic Nuclear Engineering, Allyn and Bacon Inc., Boston, (1968).
7. S. Glasstone and M. C. Edlund, The Elements of Nuclear Reactor Theory, D. Van Nostrand Company Inc., Princeton, New Jersey, (1960).
8. D. H. Stoddard and H. E. Hootman, <sup>252</sup>Cf Shielding Guide, Dupont - Savannah River Laboratory, Aiken, South Carolina, (March, 1971).
9. Paul N. Stevens, et al, Weapons Radiation Shielding Handbook.  
Chapter 3. Methods Calculating Neutron and Gamma-Ray Attenuation, Oak Ridge National Laboratory, Oak Ridge, Tennessee, (April, 1971).
10. Jere P. Nichols, "Design Data for Cf-252 Neutron Source Experiments", Nuclear Applications, vol. 4, (June, 1968).



11. E. J. Landry, "Discrete Ordinates Treatment of a Small Subcritical Assembly", M. S. Thesis, Louisiana State University, (August, 1972).
12. Donald J. Hughes and John A. Harvey, Neutron Cross Sections, Brookhaven National Laboratory, Upton, New York, (July 1, 1955).
13. Private communications with Dr. Ben Magurno, National Neutron Cross Section Center, Brookhaven National Laboratory, New York.
14. R. L. Heath, Scintillation Spectrometry Gamma-Ray Spectrum Catalogue, Phillips Petroleum Company, Idaho Operations Office, vol. 1 (1964).

## APPENDIX A

### DETERMINATION OF IRRADIATION VESSEL DIMENSIONS

The volume of the annular sample is given by equation (2-1). The minimum moderator height has been set at 1.7 inches with an allowable height variation of 0.5-inch. For the maximum and minimum moderator radius the values of 20-inches and 0.375-inch were chosen. These are the ideal variations which are to be used to determine the vessel radius and the corresponding constant volume required.

Since the volume is to remain constant the vessel radius can be determined by simultaneously solving two equations resulting from substitution of the maximum and minimum dimensions. Thus,

$$V = [(r_o)^2 - (2)^2] \tag{A-1}$$

substituting  $h_{\max}$  and the maximum moderator radius, and

$$V = [(r_o)^2 - (3/8)^2] \tag{A-2}$$

substituting the minimum values. Solving simultaneously  $r_o = 4.138$ -inches

The corresponding volume is,

$$V = [(4.138)^2 - (2)^2] \tag{A-3}$$

which yields a volume equal to 1486 milliliters.

After Plexiglas was selected as the construction material, it was found that the largest diameter vessel was 6.508-inches. With this radius the corresponding volume was

$$V = [(6.508)^2 - (3/8)^2] = 913.9 \text{ ml} \tag{A-4}$$

To simplify measurements 900 milliliters was selected as the vessel volume. To do this, the minimum moderator radius would have to be changed. Solving for this value, using 900 milliliters as the sample volume yielded

0.547-inches as the minimum moderator radius. The corresponding variation in height was 2.577-inches.

EXPERIMENTAL ACTIVATION

The following calculation will be for activating Copper-64 as a target material used in the experiment. The target material used was Copper-64 with a half-life of 12.8 hours. The activation cross-section for Copper-64 is 0.43 barns. The neutron flux is 10<sup>14</sup> neutrons/cm<sup>2</sup>-sec. The target area is 10 cm<sup>2</sup>. The target thickness is 0.547 inches. The activation rate is 1.4 x 10<sup>10</sup> atoms/sec. The number of atoms after 10 hours is 1.2 x 10<sup>11</sup> atoms. The activity is 1.2 x 10<sup>11</sup> decays/sec. The activity is 1.2 x 10<sup>11</sup> Bq.

From Table 11 the activation cross-section for Copper-64 is 0.43 barns. The neutron flux is 10<sup>14</sup> neutrons/cm<sup>2</sup>-sec. The target area is 10 cm<sup>2</sup>. The target thickness is 0.547 inches. The activation rate is 1.4 x 10<sup>10</sup> atoms/sec. The number of atoms after 10 hours is 1.2 x 10<sup>11</sup> atoms. The activity is 1.2 x 10<sup>11</sup> decays/sec. The activity is 1.2 x 10<sup>11</sup> Bq.

The activation rate is 1.4 x 10<sup>10</sup> atoms/sec. The number of atoms after 10 hours is 1.2 x 10<sup>11</sup> atoms. The activity is 1.2 x 10<sup>11</sup> decays/sec. The activity is 1.2 x 10<sup>11</sup> Bq.

$$A = N \lambda$$
  
$$N = \frac{A}{\lambda}$$
  
$$N = \frac{1.2 \times 10^{11} \text{ decays/sec}}{0.054 \text{ sec}^{-1}}$$
  
$$N = 2.2 \times 10^{12} \text{ atoms}$$

For Cu-64  $\lambda = 0.054 \text{ sec}^{-1}$  for 12.8 hr half life.  
$$N = \frac{A}{\lambda} = \frac{1.2 \times 10^{11} \text{ decays/sec}}{0.054 \text{ sec}^{-1}} = 2.2 \times 10^{12} \text{ atoms}$$

To which the activity is 1.2 x 10<sup>11</sup> decays/sec.

APPENDIX B

CALCULATION OF EXPECTED DOSE RATES FROM  
EXPERIMENTAL ACTIVATIONS

The method of calculation will be shown using Copper-64 as an example. Since the target material used contained both Copper-63 and Copper-65, both Copper-64 and Copper-66 will be produced. The decay schemes indicate that 19% of all disintegrations for Copper-64 produce 0.51 MeV gammas and 9% of all disintegrations produce a 1.04 MeV gamma for Copper-66. The dose received from pure  $\beta^-$  decay with no accompanying gamma is negligible through the 0.25 inch Plexiglas wall of the vessel.

From Table III the theoretical activity yields for Copper-64 and Copper-66 are 0.063 and 0.012 millicuries per gram. For an activation of 2 hours Cu-66 will be saturated but the saturation factor for Cu-64 will only be 0.103.

The dose rate is given by

$$\dot{D} = (\phi)(\mu)(E_{\gamma})(\rho) \quad (B-1)$$

in which

$$\phi = \frac{\text{Source Strength}}{4\pi R^2} = \text{Photons/sec.}$$

$\mu$  = energy absorption coefficient

$E_{\gamma}$  = gamma energy (MeV)

$\rho$  = density of material (tissue = 1g/cc)

For Cu-64 and  $\mu = 0.033 \text{ cm}^2/\text{gm}$  for a 0.51 MeV gamma,

$$\dot{D} = \frac{(0.063)\text{mci/gm} (3.7 \times 10^7)\text{dps/mci} (0.19) (0.033) (0.51) (1)}{4\pi(1)^2} \quad (B-2)$$

in which the radius is set equal to one centimeter.

This yields a dose rate of  $\dot{D} = 34$  mR/hr.

For Cu-66 and  $\mu = 0.03$  cm<sup>2</sup>/gm for a 1.04 MeV gamma,

$$\dot{D} = 5.3 \text{ mR/hr.}$$

Therefore the total expected dose rate at saturation is 39.3 mR/hr for each gram of copper used in the sample. For an irradiation time of two hours the saturation factor is 0.103. The dose rate which should be observed if the sample were a point source of this strength is therefore 21 mR/hr.

The expected dose rates for Na-24, In-116m and Mn-56 from similar calculations were 483 mR/hr, 2.4 R/hr, and 1.63 R/hr, respectively.

The actual dose rates observed were 3 mR/hr, 25 mR/hr, 65 mR/hr, and 200 mR/hr for Cu-64, Na-24, Mn-56 and In-116m respectively.

The reduction is caused by attenuation from the sample volume and the fact that the sample was a distributed rather than point source of radiation. The measurements were made at the surfact of the vessel which further decreases the dose rate because of the inverse square law for radiation.



APPENDIX C

ANISN AND DOT CALCULATIONS OF THERMAL FLUX

Distance (cm.)	ANISN (H <sub>2</sub> O)	ANISN (CH <sub>2</sub> )	Distance (cm.)	DOT (H <sub>2</sub> O)
0	3.18 x 10 <sup>8</sup>	4.84 x 10 <sup>8</sup>	0.32	3.22 x 10 <sup>8</sup>
1	3.20 x 10 <sup>8</sup>	4.84 x 10 <sup>8</sup>	1.08	3.08 x 10 <sup>8</sup>
2	3.06 x 10 <sup>8</sup>	4.51 x 10 <sup>8</sup>	1.95	2.81 x 10 <sup>8</sup>
3	2.80 x 10 <sup>8</sup>	3.93 x 10 <sup>8</sup>	2.81	2.45 x 10 <sup>8</sup>
4	2.45 x 10 <sup>8</sup>	3.27 x 10 <sup>8</sup>	3.70	2.05 x 10 <sup>8</sup>
5	2.10 x 10 <sup>8</sup>	2.45 x 10 <sup>8</sup>	4.46	1.70 x 10 <sup>8</sup>
6	1.75 x 10 <sup>8</sup>	1.98 x 10 <sup>8</sup>	5.06	1.45 x 10 <sup>8</sup>
7	1.45 x 10 <sup>8</sup>	1.31 x 10 <sup>8</sup>	5.82	1.18 x 10 <sup>8</sup>
8	1.12 x 10 <sup>8</sup>	1.07 x 10 <sup>8</sup>	6.71	9.00 x 10 <sup>7</sup>
9	8.89 x 10 <sup>7</sup>	7.48 x 10 <sup>7</sup>	7.57	6.88 x 10 <sup>7</sup>
10	6.95 x 10 <sup>7</sup>	5.38 x 10 <sup>7</sup>	8.46	5.18 x 10 <sup>7</sup>
			9.21	4.02 x 10 <sup>7</sup>
			9.82	3.30 x 10 <sup>7</sup>

## APPENDIX D

### CALCULATION OF EXPERIMENTAL EFFICIENCIES

#### AND EXPERIMENTAL ACTIVATION YIELDS

For the efficiency determinations the "peak area" method was used. For radioisotopes having compton contribution in the photopeak of concern, the compton contribution must be subtracted out. The radioisotopes copper-64, sodium-22, sodium-24, indium-116m and manganese-56 are included in this group. For radioisotopes in which the photopeak of interest has very little compton contribution, the total peak area can be used. Cesium-137 and cobalt-60 are in this category.

To obtain the experimental peak efficiency curve, Co-60, Cs-137 and Na-22 standard sources were counted. For Co-60 and Cs-137 the total areas under the 1.33 MeV and 0.66 MeV photopeaks were corrected for background and divided by the activity of the standard source ( $\gamma\text{-sec}^{-1}$ ).

For Cs-137, 9.3% of the 0.66 MeV gammas given off are lost to internal conversion. This had to be taken into account in the efficiency determination. For Na-22, the 0.51 MeV gamma from positron annihilation was counted. The number of positron emissions is equal to 90% of the 1.28 MeV gamma activity of the standard source. The compton contribution must be subtracted from the 0.51 MeV photopeak area.

For the determination of experimental activity yields the compton contribution was subtracted from the area of the photopeak of concern. A typical gamma spectrum obtained for a Cu-64 sample is shown in Figure 15. The extrapolated efficiency and gamma abundance were divided into the total counts less the compton contribution and background to obtain the

activity of the two milliliter aliquot. From this the activity of the entire sample was determined and divided by the weight of target isotope in the sample. This yielded the activity per gram which was then extrapolated to saturation.



Faint, illegible text at the bottom of the page, possibly a caption or a reference.

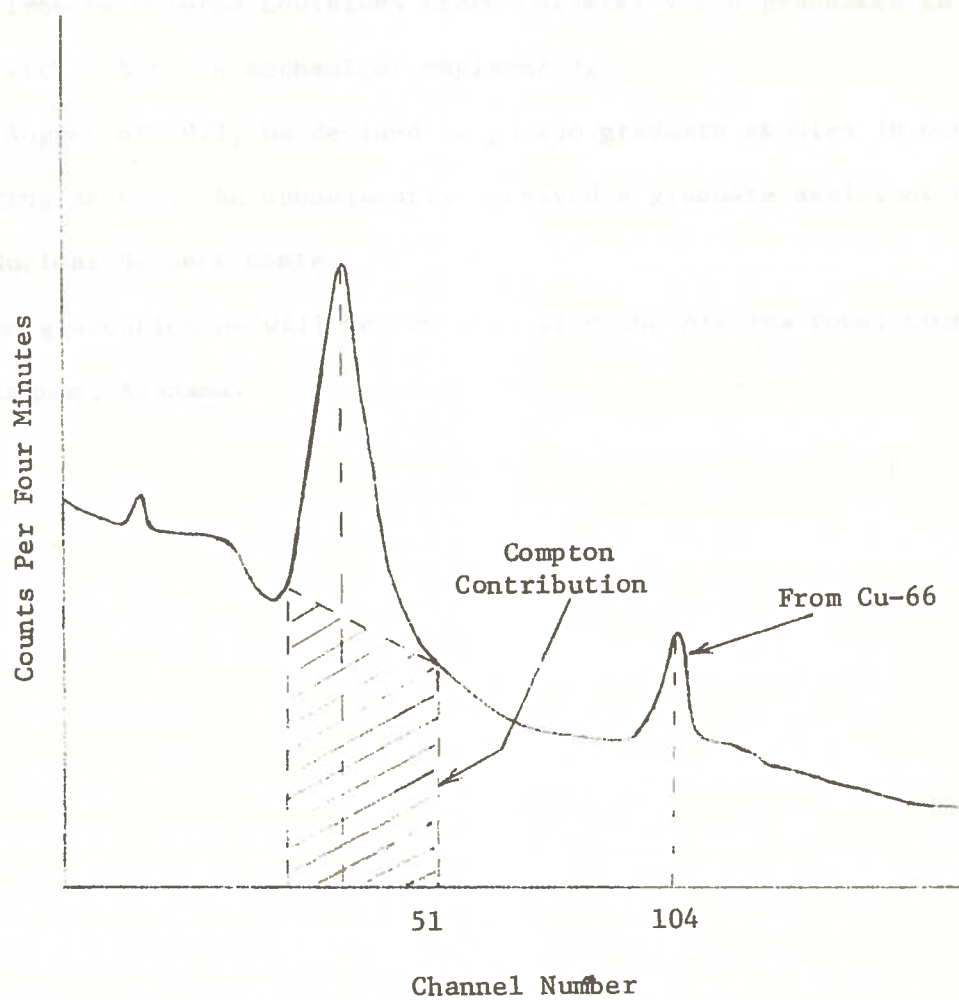


FIGURE 15. Typical Gamma Spectrum Obtained for Cu-64 Sample

VITA

Rodney D. Rogers was born on August 20, 1948, in Lafayette, Louisiana. He attended Lafayette High School in Lafayette, and graduated in 1966.

In 1966 he entered Louisiana State University and graduated in May of 1971 with a B.S. in mechanical engineering.

In August of 1971, he decided to pursue graduate studies in nuclear engineering at LSU. He subsequently received a graduate assistantship in the Nuclear Science Center.

Upon graduation he will be employed with the Alabama Power Company in Birmingham, Alabama.

*Handwritten signatures and notes:*  
W. L. ...  
M. ...  
C. ...

Approved for Publication:

June 29, 1972



EXAMINATION AND THESIS REPORT

Candidate: Rodney Dale Rogers

Major Field: Nuclear Engineering

Title of Thesis: Production of Radioisotopes For Medical and Industrial  
Uses With Californium-252.

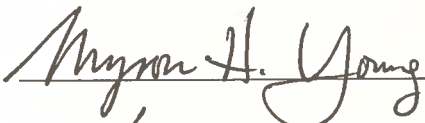
Approved:

  
Major Professor and Chairman

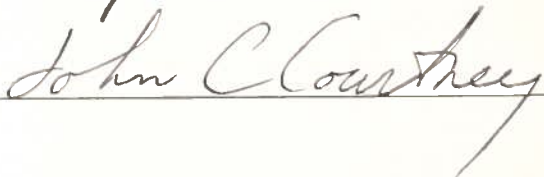
  
Dean of the Graduate School

EXAMINING COMMITTEE:









Date of Examination:

June 29, 1973